Title Page

Targeting autoimmunity in Rheumatoid Arthritis with nanoparticles displaying Liprin-1 peptide

Authors:

Anthony Rosa[1], Alessia Raneri[2], Michela Campolo[3], Emanuela Esposito[3], Elisa Gecchele[1], John Edward Butler[4], Julian K-C. Ma[4], Nidhi Sofat[4], Santiago Figueira[5], Denise Pivotto[2], Alison McCormick[6], Elena Bartoloni[7], Roberta Zampieri[1], Linda Avesani[2,*]

Affiliations:

[1]Diamante SB srl, Viale del Lavoro, 33. 37135 Verona (Italy)

[2]Dipartimento Biotecnologie, Università di Verona, Strada Le Grazie 15. 37134 Verona (Italy)

[3] Department of Chemical, Biological, Pharmaceutical and Environmental Sciences; University of Messina. Viale Ferdinando Stagno D'Alcontres, 31- 98166 Messina (Italy)

[4]Institute for Infection and Immunity, School of Health and Medical Sciences, City St. George's University of London, Cranmer Terrace, London SW17 0RE (UK)

[5]Palobiofarma S.L., Carretera Pamplona 1 31191 Galar (Spain)

[6] Department of Chemical Engineering, University of California, 3001 Ghausi Hall, Davis, CA (USA)

[7] Department of Internal Medicine, University of Perugia (Italy)

**Corresponding author. Email: linda.avesani@univr.it.*

One Sentence Summary: *Plant-made nanomaterials induce tolerance in arthritis models via repeated IV dosing that triggers a regulatory immune response.*

Abstract

Nanoparticle-based strategies offer a promising tool for inducing antigen-specific immune tolerance across various autoimmune conditions, by acting as master switch to turn-off the autoimmune response. Building on our previous work demonstrating the therapeutic potential of plant-made nanoparticles in rheumatoid arthritis, we present a systematic evaluation of key parameters—including dosing regimen, route of administration, and immunization schedule—to optimize both efficacy and safety. We developed virus-based nanomaterials expressing Tomato Bushy Stunt Virus (TBSV) nanoparticles engineered to display the immunodominant Liprin-1 peptide in the *Nicotiana benthamiana* plant platform. The mechanisms responsible for the observed protective effects against rheumatoid arthritis were also investigated.

Our findings highlight the critical role of repeated intravenous administration and precise dosing in promoting regulatory T cell (Treg) induction and cytokine modulation. Furthermore, we dissected the individual contributions of the Liprin-1 peptide and the viral capsid scaffold in driving immune tolerance.

These results support the potential of plant-derived nanoparticles as a versatile and effective platform for antigen-specific immunotherapy, with rheumatoid arthritis serving as a proof-of-concept model for broader applications in the field of autoimmunity.

Main Text

INTRODUCTION

Rheumatoid arthritis (RA) is a chronic, progressive and debilitating autoimmune disease characterized by the malfunction of various immune cell types and signaling network, resulting in an improper tissue repair process that primarily damages the joints but also affects the lungs and the vascular system[1]. In 2020, an estimated 17.6 million people worldwide had RA and this number is projected to increase to 31.7 million by 2050 based on forecasted change in population age[2].

Since the first treatments for symptomatic relief (non-steroidal anti-inflammatory drug and glucocorticoids), RA treatment has evolved to include disease modifying anti-rheumatic drugs (DMARD), ranging from methotrexate to advanced biological and targeted synthetic DMARDs, yet these treatments still cannot fully address the underlying immune disorders, requiring lifelong use with the possibility of severe adverse effects[3].

For decades, numerous studies for autoimmune diseases therapy, have aimed to restore tolerance, which is the ability of the immune system to ignore self-antigens while appropriately attacking foreign ones[4]. Tolerance induction may be achieved either by 1) anergy or deletion of specific-autoreactive T-cells or by 2) converting autoreactive T cells to a Treg phenotype[5]. The ultimate goal of the latter approach is to re-program autoreactivity to induce bystander immunoregulation by the capacity of one or a few autoreactive regulatory T- and/or B-cell specificities, which will ultimately blunt the activation of non-cognate effector lymphocytes. A major advantage of this "active" approach, defined as Antigen-specific Immunotherapy (ASI), is that sustained activation and expansion of regulatory cells targeting specific epitopes should be able to block the recruitment and activation of all other adaptive and innate immune cells that take part in the disease process[6].

Several products that have shown promising results are now at various stages of the clinical development pipeline[3]; among these, nanoparticles hold significant promise for development, due to a better understanding of their mechanisms of action in different autoimmune diseases settings[7]. In tolerance induction, nanoparticles using inorganic and/or organic materials can act as vehicles for drug and/or antigen delivery to phagocytes, as well as direct T-cell targeting compounds[8]. By specific design, the structural properties of nanomaterials can contribute to the pharmacokinetic and pharmacodynamics of a target compound, becoming an essential ingredient of the final product rather than an inert component[6].

We previously demonstrated in preclinical studies that plant-made Virus Nano-Particles (VNPs) can be successfully used to induce tolerance both for autoimmune diabetes prevention and for RA treatment[9]; VNPs, derived from two distinct plant viruses, were genetically engineered to display immunodominant peptides related to the target autoimmune diseases on their outer surface. They were then propagated in *Nicotiana benthamiana* plants through a rapid expression system[9]. Notably, commercial approval was granted for the first time in 2023 for a COVID-19 VLP vaccine produced using the same bio factory, *N.benthamiana*[10]. The workflow exploited enables safe production of high titers of monodispersed VNPs in short timeframes, thus paving the way for their future advancement as a therapy for tolerance induction in autoimmune diseases. We recently established a GMP-compliant facility for the manufacturing of

clinical-grade VNPs meant to progress to a first in human (FIH) clinical study of the safety of the particles[11].

Starting from this first proof-of-concept of the use of plant-made VNPs for tolerance induction, we further explore their therapeutic potential, namely, TBSV.pLip, in RA treatment by pre-clinical studies specifically designed to determine their pharmacological activity. Furthermore, the mode of action of TBSV.pLip in a pre-clinical model has been established.

RESULTS

Nanoparticles manufacturing in a TBSV/plant-based system

TBSV WT and TBSV.pLip virus nanoparticles (VNPs) were produced in *N. benthamiana* plants, following previously established protocols[8] and a recently optimized production workflow[11].

VNPs were purified from infected leaf tissue and quantified via enzyme-linked immunosorbent assay (ELISA). VNPs were then characterized by agarose gel electrophoresis and Dynamic Light Scattering (DLS) to assess integrity and size distribution (Figure 1A–B). DLS analysis detected no significant difference in hydrodynamic radius between TBSV.pLip and TBSV WT (Figure 1B). Extraction of nanoparticles occurred under sterile conditions and endotoxin levels was below the acceptable standard of 1.50 EU/ml[12].

Zeta potential measurements revealed that the surface charge of the VNPs is negative, showing an average of -10.67 mV for TBSV.pLip and -9.05 mV for TBSV WT (Figure 1B). Transmission electron microscopy (TEM) analysis confirmed that both formulations exhibited uniform spherical morphology, (Figure 1C). Modelling of the TBSV CP monomer indicates that the surface-exposed β-sheet motifs are highly conserved, except for the Liprin-1 peptide (pLip), which is sequestered within the interstitial regions at subunit interfaces (Figure 1D). These findings support experimental data (Figure 1B-C), indicating that TBSV.pLip particles, despite incorporation of the peptide, do not exhibit increased dimensions compared to TBSV WT.

Induction of arthritis by Liprin-1 peptide

Since RA patients, regardless of RF positivity, produce autoantibodies against the Liprin-1 peptide[13], we investigated whether Liprin-1 peptide immunization induces arthritis in mice. The dodecamer Liprin-1 peptide (ASVLANVAQAFE) shares 100% homology with the 3 human isoforms Liprin-alpha-1 (NP_803172.1, NP_003617.1, NP_001364935.1) and the 2 mice isoforms (NP_001182015.1, NP_001028491.1).

Male DBA/1J 8-weeks old mice were intradermally injected either with Liprin-1 peptide (0.2 mg/mouse) and chicken type-II Collagen (0.1 mg/mouse) both emulsified in CFA and boosted on day 21 with the same dose (Figure 2A). Within a week post-boost, mice developed progressive inflammatory arthritis (Figure 2B, Supplementary Figure 1). Clinical scores in Liprin1-induced arthritis (LIA) mice were statistically comparable to those in collagen-induced arthritis (CIA) mice throughout the study (Figure 2B, Supplementary Figure 1).

60 days after injection, mice with CIA and LIA showed a significant increase in synovial membrane inflammation, cartilage and bone erosion (Figure 2C-D, Supplementary Figure 1) in comparison to the sham group.

LIA and CIA in mice is associated with a significant increase of most pro-inflammatory cytokines (MCP-1, IL-17, IL-1b, IL-6, IL-12 p60) in sera compared to sham (Figure 2E, Supplementary Figure 1) with IL-17 and MCP-1 being the most abundant response and with a concomitant decrease in the population of Treg cells (Figure 2F, Supplementary Figure 1).

Administration routes for tolerance induction

In most preclinical approaches to tolerance induction, the route of administration is not systematically compared. In this study, we evaluated the impact of different administration routes on the ability to halt the progression of RA clinical signs in CIA mice. We previously demonstrated that seven intraperitoneal (i.p.) injections administered five days apart were effective in treating arthritis in this model[9]. Using the same treatment schedule (Figure 3A), we compared four administration routes: intraperitoneal (i.p.), subcutaneous (s.c.), intravenous (i.v.), and oral (p.o.).

Clinical scoring revealed that all tested administration routes led to a statistically significant reduction in cumulative disease scores in comparison to CIA, with i.v. treatment showing the highest effect, statistically comparable to dexamethasone (Figure 3B, Supplementary Material 1).

Histological analysis at the end of the treatment confirmed the superior performance of i.v. administration in restoring ankle-joints integrity, based on reduced synovial hyperplasia, pannus formation, cellular infiltration and cartilage erosion (Figure 3C-D, Supplementary Material 1). Pro-inflammatory cytokines levels in sera were most affected by i.v. and i.p. administrations; in particular, MCP-1 displayed a significant greater reduction than those observed with dexamethasone (Figure 3E, Supplementary Material 1). CD4+CD25+Foxp3+ regulatory T cells (Treg), which play a crucial role in preventing chronic inflammatory and autoimmune diseases by suppressing autoreactive T cells, were significantly increased in splenocyte from CIA mice treated via i.v. injection of TBSV.pLip. In contrast, i.p. administration resulted in a modest increase in Treg activation, while other routes did not produce statistically significant changes compared to CIA untreated mice (Figure 3F, Supplementary Material 1).

Administration Scheme for Tolerance Induction

Given the unique characteristics of our nanoparticles in comparison to others previously used in the autoimmune context[15], we wanted to establish the optimal number of i.v. injections required to effectively halt arthritis progression in our animal model by a dose number escalation scheme (Figure 4A).

Treatments with 2, 4 and 7 i.v. injections of 50 µg TBSV.pLip resulted in a significant reduction in clinical scores compared to the CIA control group (Figure 4B, Supplementary Material 1). These same treatment groups also exhibited markedly lower ankle-joints lesion scores relative to the CIA group (Figure 4 C-D, Supplementary Material 1).

Serum analysis of pro-inflammatory chemokines and cytokines revealed that both the 4 and 7 i.v. TBSV.pLip treatments significantly decreased MCP-1, IL-6, TNF-α, IL-1β and IFN-γ compared to the CIA group (Figure 4E, Supplementary Material 1). The group receiving 1 or 2 i.v. injections of TBSV.pLip showed no reduction in the analyzed cytokines (Figure 4E, Supplementary Material 1). Furthermore, splenocytes analysis demonstrated that mice treated with 4 and 7 i.v. doses of TBSV.pLip restored the percentage of CD4+CD25+Foxp3+ regulatory T cells to levels comparable with healthy controls (Sham Group). A moderate significative increase in this cell population was also observed in the group treated with 2 i.v. injections, relative to the CIA group (Figure 4F, Supplementary Material 1).

Furthermore, the 4 and 7 i.v. groups were analyzed at 60 days for the accumulation of TBSV.pLip particles in the organs, the two groups were selected because they had the same number of hours post the last TBSV.pLip i.v. injection (48 hours); the data showed high biological variability and no statistically significant differences were observed among the organs tested (Supplementary Figure 2), all characterized by low values of % Injected Dose (ID)/g of tested tissue.

Dose-Effect Relationship of VNPs efficacy

Subsequently, we investigated the dose-response relationship by administering four i.v. doses—5, 20, 50, and 200 µg—every 10 days to assess their ability to induce tolerance. This approach allowed us to evaluate a broader range of concentrations and assess their efficacy in triggering a tolerogenic response. To better approximate the clinical course of RA in humans and to assess preliminary indicators of tolerance durability, we extended the experimental timeline relative to previous studies (Figure 5A).

Notably, mice receiving four i.v. doses of 50 or 200 µg TBSV.pLip exhibited a markedly significant improvement in clinical scores, whereas lower doses (5 and 20 µg) failed to produce benefits compared to the CIA control group (Figure 5B, Supplementary Material 1). After 70 days, histological analysis of ankle joints revealed markedly reduced tissue damage in the 50 and 200 µg treatment groups relative to CIA controls (Figure 5C-D, Supplementary Material 1).

Correspondingly, serum levels of inflammatory cytokines were significantly decreased in mice treated with 50 and 200 µg TBSV.pLip, as well as in the dexamethasone reference group. A moderate but statistically significant reduction was observed in the 20 µg group, while the 5 µg group showed no significant difference from CIA controls (Figure 5E, Supplementary Material 1).

This anti-inflammatory profile was mirrored in splenic $CD4^{+}CD25^{+}FoxP3^{+}$ regulatory T-cell populations, which were markedly expanded in the 50 and 200 µg groups and in dexamethasone-treated mice. The 20 µg-group showed partial restoration, whereas no change was detected in the lowest dose group (Figure 5F, Supplementary Material 1).

Splenectomy does not impact tolerance induction in mice

To elucidate the mechanistic contribution of the spleen in tolerance induction, we compared two groups—splenectomized and non-splenectomized mice—using the experimental protocol corresponding to the four-injection scheme previously used and illustrated in Figure 6A. Splenectomized animals exhibited comparable susceptibility to CIA as control mice, as evidenced by similar clinical scores (Figure 6B, Supplementary Material 1), histopathological assessments (Figure 6C-D, Supplementary Material 1) and serum profiles of most pro-inflammatory cytokines (Figure 6E, Supplementary Material 1), thus confirming the resilience of the model strain to splenectomy, as previously described[16].

Importantly, mice receiving 4 i.v. doses of 50 µg of TBSV.pLip demonstrated a significant reduction in both clinical and histological scores (Figure 6B-D, Supplementary Material 1) regardless of splenectomy status, when compared to untreated CIA controls. Moreover, analysis of serum cytokines revealed a significant decrease in pro-inflammatory mediators in both splenectomized and non-splenectomized groups treated with TBSV.pLip, mirroring the immunosuppressive profile observed in dexamethasone-treated reference animals (Figure 6E, Supplementary Material 1). No antibody reactivity was detected against Liprin-1 peptide in all the groups (Figure 6F).

Impact of the viral shell on tolerance induction

In order to evaluate the immunomodulatory profile of the TBSV viral shell, we first compared the effects of seven intravenous (i.v.) injections of TBSV WT and TBSV.pLip (Supplementary Figure 3). TBSV WT treatment resulted in a markedly reduced therapeutic effect across clinical scores, histological assessments, and cytokine/chemokine profiles compared to TBSV.pLip (Supplementary Figure 3). We hypothesize that the discrepancy with previous findings, that showed a partial immunomodulation by TBSV WT[9], may be attributed to differences in administration route (i.p. vs i.v.), which influences systemic immunomodulation. Additionally, the current study employed a larger sample size (n = 10) compared to the earlier work (n = 3), increasing statistical robustness.

To further dissect the mechanism of action, we evaluated the optimized treatment protocol—four i.v. injections of 50 µg VNPs—in CIA mice, comparing TBSV.pLip and TBSV WT (Figure 7A). Mice treated with TBSV.pLip showed significant improvement in clinical parameters relative to CIA controls, whereas TBSV WT treatment did not yield any observable benefit (Figure 7B, Supplementary Material 1). Histological analysis corroborated these findings, with reduced joint damage in the TBSV.pLip group and no significant improvement in the TBSV WT group compared to CIA group (Figure 7C–D, Supplementary Material 1).

Assessment of pro-inflammatory cytokines revealed overall no significant reduction in the TBSV WT group compared to CIA (except for IL-1β and IL-6), while TBSV.pLip treatment confirmed a robust decrease in all the inflammatory markers considered (Figure 7E, Supplementary Material 1). To explore the anti-inflammatory response, we quantified serum levels of IL-4, IL-10, and TGF-β. TBSV.pLip treatment significantly elevated all three cytokines, with the most pronounced effect observed for TGF-β and IL-4 (Figure 7F, Supplementary Material 1).

Flow cytometric analysis of splenocytes demonstrated a substantial restoration of $CD4^+CD25^+Foxp3^+$ regulatory T cells in the TBSV.pLip-treated group, in contrast to the CIA group and TBSV WT-treated mice, which showed no significant change (Figure 7G, Supplementary Material 1). Immunofluorescence co-labelling of mesenteric lymph nodes revealed a significant increase in tolerogenic dendritic cells ($CD11c^+$/PD-$L1^+$) in the TBSV.pLip group compared to CIA controls. The CIA group exhibited elevated levels of $CD11c^+$/PD-$L1^+$ cells relative to sham, consistent with dendritic cell activation following collagen immunization. Notably, TBSV.pLip treatment further enhanced the presence of tolerogenic dendritic cells, suggesting a role in promoting immune tolerance. In contrast, TBSV WT treatment did not alter dendritic cell populations compared to CIA (Figure 7H, Supplementary Material 1). No differences in antibody reactivity were detected against Liprin-1 peptide in the different groups (Figure 7I).

DISCUSSION

Despite notable progress in developing disease-modifying therapies for autoimmune disorders[17], long-term clinical success depends on restoring durable, antigen-specific immune tolerance, as current treatments can achieve remission but typically require prolonged therapies accompanied by regular monitoring and potential side-effects. Antigen-specific immunotherapy (ASI) has emerged as a promising strategy to selectively suppress pathogenic immune responses while preserving essential functions such as antimicrobial defense and tumor surveillance[1518]. In the context of rheumatoid arthritis (RA), ASI represents a compelling alternative to broadly immunosuppressive treatments. Although various approaches—including cell-based therapies and autoantigen-loaded liposomes—have shown

encouraging results[19], none have yet translated into approved therapies for RA. The challenge of achieving sustained, antigen-specific tolerance in a clinically viable format remains unmet.
In this study we aimed to define an optimal strategy for an ASI using a novel plant-made nanomaterial, with preliminary efficacy in reversing RA pathology that was previously demonstrated in a disease animal model by our group[9].
The nanoparticles used are based on the plant virus TBSV, genetically modified to display a dodecameric peptide derived from human Liprin-1, previously identified as a target of autoantibodies in RA patients[13]. Structurally, each nanoparticle is a ~30 nm sphere displaying 180 peptide copies on its outer shell, with an estimated intramolecular spacing of 6.4 nm (based on the PDB deposited model), and a net negative surface charge as indicated by the zeta potential at physiological pH—features that align with design principles commonly adopted for nanoparticles intended for tolerance induction[20]. The production of these particles relies on a robust bioprocess that enables consistent generation of TBSV-derived nanomaterials. Importantly, TBSV.pLip preserves key physicochemical attributes of wild-type particles, including size and zeta potential. This consistency suggests that the engineered particles mimic the native architecture without compromising particles stability.

Firstly, to elucidate the role of the recently described Liprin-1 peptide[13] in the disease onset, we demonstrated that Liprin-1 induced inflammatory arthritis (LIA) shares clinical, histological and immunological features with RA, similarly to collagen. Our results suggest that Liprin-1 peptide is robustly arthritogenic in mice and that LIA is mediated by autoreactive T cell responses. Our study highlights that arthritis development in LIA DBA/1j mice is T-cell mediated in the absence of antibody towards the peptide as previously observed with other immunodominant and arthritogenic peptides[21]. Our findings indicate that the Liprin-1 peptide exhibits key features of an autoantigen involved in disease onset, making it an optimal target for antigen-specific immunotherapy (ASI) in RA.

To optimize the use of TBSV.pLip nanoparticles within a tolerance induction strategy, we systemically compared the effects of modifying individual variables on both efficacies, Treg induction and pro-inflammatory cytokines downregulation compared to dexamethasone given every other day.

In this regard, i.v. administration resulted to be the most efficacious route of delivery, compared to s.c, i.p and o.p. As previously demonstrated, nanoparticles with diameter below 500 nm administered via i.v. injection exhibit superior bioavailability and enable precise dosage control, outperforming other administration routes in promoting immune tolerance[22]. Mixed administration routes combining intravenous (i.v.) and subcutaneous (s.c.) injections were also tested but proved inferior in terms of clinical outcomes compared to the use of i.v. alone (Supplementary Figure 4), which inhibited RA symptoms equivalent to dexamethasone treatment.

Administration protocols for tolerance induction vary widely across preclinical studies. In the experimental autoimmune encephalomyelitis (EAE) model, i.v. injection of nanoparticles is typically performed as a single dose [22,23,24,25]. In contrast, peptide-MHC based nanomedicine and peptide/autoantigen-based approaches in different animal models often require multiple administrations, ranging from 3 to 10 injections [26,27,28]. Our results demonstrate that the number of i.v. injections is a key determinant for inducing immune tolerance, with four and seven administrations representing the most effective regimens. Experimental designs across reported preclinical studies further show that the tolerance profile—characterized by Treg induction and downregulation of pro-inflammatory cytokines—remains stable over time, up to 12 days post-treatment. This supports the hypothesis that the observed effect is primarily dependent on the number of administered doses, rather than the interval between the final dose and the time of sacrifice. This is clearly illustrated by comparing the two preclinical studies presented in Figures 4 and 5: in Figure 5, both the 4-dose and 7-dose i.v. groups were sacrificed 12 days after the last i.v. injection, and exhibited sustained tolerance markers; similarly, in Figure 4, the 2-dose

i.v. group—also sacrificed 12 days post-treatment—showed a markedly reduced tolerance profile, reinforcing the dose-dependent nature of the observed effect.

To enhance the translational potential of our approach, we further investigated the 4-doses protocol by evaluating the optimal quantity of nanoparticle to be injected.

Precise modulation of pathogenic $CD4^+$ T-cell responses require careful dosing optimization. In the EAE model, tolerance induction has been shown to be dose-dependent, with higher peptide doses (8 µg) eliciting stronger effects than lower doses (0.8 µg), although subcutaneous administration of high doses also triggered inflammatory cytokine production in TCR transgenic mice[29]. In murine models, peptide doses typically range from micrograms to milligrams, with distinct mechanisms of action across this spectrum[30], indicating that a threshold plasma concentration of tolerogen may be necessary to establish systemic tolerance [30]. Our strategy leverages a low-dose regimen enhanced by the intrinsic adjuvancy of the viral nanoparticle shell. We systematically evaluated dosing parameters, maintaining a consistent schedule, with total VNP doses ranging from 20 to 800 µg—corresponding to 0.64 to 25.6 µg of Liprin-1 peptide and 1.68×10^{12} to 6.72×10^{13} nanoparticles. A clear dose-dependent effect was observed, with higher doses (50 µg and 200 µg) outperforming lower ones (5 µg and 20 µg). Notably, the 50 µg dose yielded slightly better clinical scores and reduced levels of specific pro-inflammatory cytokines than the higher dose (200µg). Intravenous injections of 50 µg TBSV.pLip effectively protected both CIA and LIA mice from arthritis development (Figures 3-4 and Supplementary Figure 5), confirming the key role of Liprin-1 as an immunodominant peptide with superior efficacy in inducing immune tolerance.

Having developed and fine-tuned a therapeutic strategy for immune tolerance induction in a murine RA model, we proceeded to investigate its potential mechanism of action, drawing on previous studies indicating that most i.v. delivered biomaterial formulations tend to accumulate in the liver and spleen, where they facilitate antigen presentation to resident antigen-presenting cells (APCs)[31].

Although previous studies have identified the spleen as a key organ for tolerance induction using antigen-linked splenic leukocytes[32], our findings in splenectomized mice suggest that, in the context of RA and TBSV-based nanomaterials, the liver plays a central key role. Previous biodistribution analysis confirmed liver accumulation of TBSV nanoparticles and their uptake by Kupffer cells[33],—known mediators of immune tolerance[34], thus we hypothesized that the liver's tolerogenic environment supports the conversion of non-Tregs into immunosuppressive Tregs, enabling systemic regulation of autoimmune responses as previously demonstrated by other groups[35],[36]. The biodistribution study here performed does not show differences in organ distribution, but it was limited to one single analysis 48 hours after the last injection of VNPs.

To further investigate the intrinsic contribution of nanoparticle structure to immunomodulatory efficacy, we conducted a comparative analysis between wild-type TBSV particles (TBSV WT) and engineered particles displaying the Liprin-1 peptide (TBSV.pLip). In our previous study[8], seven i.p. administrations of TBSV WT conferred partial protection against arthritis symptoms in the CIA model, albeit with lower efficacy than the same regimen using TBSV.pLip. Modulation of cytokine profiles was also observed, particularly with respect to TGF-β activation.

In this study i.v. administration of nanoparticles conferred specific protection against the development of RA exclusively in mice treated with TBSV.pLip. In contrast, animals treated with WT TBSV showed no significant changes in cytokine profiles, nor evidence of tolDC or Treg induction.

Taken together, our findings support a model in which repeated and dose-controlled presentation of the immunodominant Liprin-1 peptide by TBSV viral particles in the liver and lymph nodes stimulates the expansion of tolerogenic dendritic cells (tolDCs). These cells, as proposed in other tolerance induction

studies[28], promote clonal anergy in autoreactive Th1 clones and facilitate the differentiation of regulatory T cells. Additionally, a complementary mechanism contributing to the establishment of tolerance involves the metabolic modulation of T cells through the production by activated Treg and/or tolDC of the widely described cytokines IL-10, TGF-β[37], and of IL-4.

IL-4 has been shown to play a crucial role in the suppressive function of regulatory T cells (Tregs), likely by enhancing granzyme expression[38]. As an anti-inflammatory cytokine, IL-4 also contributes to the attenuation of rheumatoid arthritis by balancing Th1 cell activity and limiting monocytic cell activation[39].

In RA, no single autoantigen has been definitively identified, and multiple autoantigens may be involved. However, here we show that arthritis induced by collagen can be halted using the single Liprin-1 autoantigen therapeutic peptide, that once displayed in a VNP context, demonstrates significant pharmacomodulating properties. Once tolerance is established, it can extend to related peptides and autoantigens within the same tissue. This suggests that tolerance induction might be sufficient to ultimately target all pathogenic T-clones.

One of the key challenges for clinical translation of this approach is determining the duration of the induced tolerance. Preliminary data in humans suggest that a single administration of antigen-specific immunotherapy (ASI) can modulate immune responses to allergens for several months[39]. We would ideally test the single dose and multiple doses therapeutic efficacy of TBSV.pLip in human patients with RA.

To support future clinical testing, we have recently established a GMP-compliant production pipeline[11], ensuring both scalability and regulatory readiness.

MATERIALS AND METHODS

Study Design

For animal studies, control and experimental treatments were administered to mice. Sample sizes were determined empirically to ensure adequate statistical power and were consistent with field standards for the techniques used in the study. Prior to treatment initiation, animals were randomized to different treatment groups based on clinical score. The number of samples and the experimental replicates is reported in the figure legends. All procedures involving animals complied with Italian regulations on the protection of animals used for experimental and other scientific purposes (DM 116/1992) as well as EU regulations (Directive legislation (EU) (2010/63/EU).

Biosynthesis and analysis of nanoparticles

The VNPs were produced and purified as previously described[9]. To confirm the presence, integrity and structure of VNPs total soluble proteins were extracted from infected leaves and analyzed by electrophoresis on agarose gel and DLS, as described[11]. After purification, VNPs were quantified by an ELISA test[11] and were analyzed manufacturer to assess endotoxin content by LAL test as described by the manufacturer (Gen Script).

Particles size (Z-Average), zeta-potential and polydispersity index (PDI) of VNPs were determined by dynamic light scattering (DLS) and electrophoretic light scattering (ELS) using a Zetasizer Pro-Blue instrument (Malvern-Panalytical, Malvern, UK) and the Malvern Zetasizer software for data analysis.

The zeta-potential was calculated using the mixed mode measurement phase analysis light scattering (M3-PALS) technique (Malvern-Panalytical, Malvern, UK). 0.5 µg/µL VNP solutions were dispensed in a folded capillary zeta cell to a final volume of 800 µL using a physiological solution (0.7% NaCl). Data were collected at 25 °C setting the refractive and absorption index to 1.45 and 0.001 respectively. Data are reported as mean ± SD of three technical replicates. All the analyses were performed by Sphera Encapsulation srl, Verona, Italy.

For TEM imaging, samples were absorbed on glow discharged (Leica EM ACE 600) 400 mesh carbon coated copper grids, and then negative stained with 2% aqueous uranyl acetate. Samples were subsequently examined with a Tecnai G2 (FEI) transmission electron microscope operating at 120 kV, and digital images were acquired using a Veleta (Olympus Soft Imaging Solutions) digital camera. Images were analyzed for diameter measurement by ImageJ.

For CP modelling, the primary TBSV and TBSV.pLip coat proteins were modelled independently using Alphafold3[40]. Proteins were aligned using ChimeraX[41] .

Mice

Male DBA/1J mice (8 weeks; Envigo, Italy) were used for these studies. Mice were housed in individual cages (two for each group) and maintained under a 12:12 light–dark cycle at 21°C ± 1°C and 50% ± 5% humidity. The animals were acclimated to their environment for 1 week and had ad libitum access to tap water and a standard rodent diet.

Induction of Arthritis

Induction of arthritis was performed by inoculation with Chicken type-II collagen with Complete Freund's adjuvant (CFA) on Day 0 (0.1 mg/0.1 mL/mouse), intradermally (ID) at the basis of the tail and boosted ID on day 21 with collagen emulsified with IFA/CFA (TBD) (0.1 mg/0.1 mL/mouse)[42]. The positive control with dexamethasone was administered orally.

Clinical and histological assessment of arthritis

Mice were assessed two times per week for redness and swelling of limbs and a clinical score from 1 to 4 (i) slight edema and erythema limited to ankle; (ii) slight edema and erythema from the ankle to the tarsal bone; (iii) moderate edema and erythema the ankle to the tarsal bone; (iv): edema and erythema from the ankle to the entire leg)[43]. At the end of the experiment, the paws from the mice were collected and prepared for hematoxylin and eosin staining (H&E) and evaluated for histological alterations. Moreover, at the end of experiment, spleen weights for all the groups were recorded.

FACS Analysis

Spleen were collected from mice, washed twice with phosphate-buffered saline (PBS), ground with two glass slides, filtered with a 200-mesh sieve, and centrifuged at 1000 rpm for 5 min; the supernatant was removed; and the precipitate was. The precipitate was held twice with PBS, centrifuged at 1000 rpm for 10 min; the supernatant was removed; and the precipitate was left. Then, 2 mL of erythrocyte lysate was added to resuspend the precipitate, incubated at room temperature for 5 min, and centrifuged at 1000 rpm for 10 min to obtain splenocytes. A single-cell suspension of splenocytes at 2×106/mL was prepared. Cells were stained with anti-CD4, anti-CD25, and anti-Foxp3 monoclonal

antibodies according to the instructions of the manufacturer. Cell events were collected on a flow cytometer and the stained CD4+CD25+Foxp3+Treg cells were analyzed using flow software[44].

Cytokine Quantification

Serum was collected and used for cytokines analysis (IL-12 p70, IL-1b, INF-γ, IL-6, MCP-1, IL17 A and TNF-α) by performing ELISA kit and following manufacturer's instructions.

ELISA for detecting anti-Liprin-1 antibodies

ELISA plates were coated with 100µl of 10µg/ml of streptavidin in carbonate buffer at pH 9.6. A standard curve was made with purified mouse IgG. After plate blocking, 1 µg/ml of biotin-Lip1 was added and incubated overnight at 4°C. Plates were washed and 1:1 serial dilutions of animal sera were added. Plates were washed and a 1:5000 dilution of anti-mouse AP- secondary antibody was added in PBS 1X +1%BSA and incubated 1 hour at 25°C. Plates were then washed and developed with pNPP 1h at 37°C.

Splenectomy

The splenectomy was performed as previously described[45]. Animals were anesthetized with 5% isoflurane and monitored until their respiratory rate dropped below 60 breaths per minute. Surgical instruments were sterilized between procedures and arranged on a sterile table along with sutures, forceps, scissors, and twisters. The abdominal skin was sterilized with iodine, and a 0.5 cm midline incision was made just below the xyphoid process. The underlying fascia was identified and incised along the same length. The spleen was mobilized from the left upper quadrant using smooth forceps and a cotton-tip applicator and brought to the midline incision. Attachments and vessels at the hilum were cauterized using an eye cautery with a heated tip, applying a vessel-preserving technique to minimize trauma and blood loss. The fascial layer was closed with 4-0 Vicryl sutures, and the skin was closed with five interrupted 4-0 Vicryl stitches using a Wire Twister. Procedures lasted approximately 5–10 minutes. Animals were kept under a heat lamp to prevent hypothermia and received 1 mL of subcutaneous saline to replace fluid losses. Postoperatively, mice were observed for several minutes and then hourly for 4 hours.

Preparation of Mouse Organs for TBSV.pLip Particle Content Analysis

Tissue samples were placed in 1.5 mL microcentrifuge tubes containing three glass beads. An extraction buffer (25 mM bicine, 150 mM NaCl, 1% Triton X-100, pH 7.6) was added at a ratio of 1:2 (w/v). Samples were homogenized for 6 seconds at maximum speed, followed by incubation on ice for 20 minutes. The homogenate was centrifuged at 5,000 × g for 10 minutes at 4 °C. The resulting supernatant was carefully collected and transferred to a new 1.5 mL microcentrifuge tube for ELISA analysis.

Statistical Analysis

All values are expressed as mean ± standard deviation (SD) of the mean of n observations. Data sets were examined by one-way analysis of variance ANOVA followed by a Bonferroni post-hoc test for multiple comparisons. Data of DLS are presented as mean +/- standard deviation. Statistical significance between

groups was determined using a two-tailed Student's t-test. A p-value< 0.05 was considered statistically significant.

FIGURE LEGENDS

Fig. 1 Virus nanoparticles characterization

(A) Agarose gel electrophoretic patterns of 1 µg of purified TBSV.pLip and TBSV WT. MM: molecular marker.

(B) Characterization of TBSV.pLip and TBSV WT by DLS evaluation, measuring size distribution by number and their Zeta Potentials. The reported data represent the mean value of 50 measurements +/- standard deviation. The data groups were compared by Student T-test. n.s.: not significant.

(C) TEM images of TBSV.pLip and TBSV WT.

(D) Structural modeling of TBSV.pLip and TBSV WT coat protein monomers. The sequence alignment shows a score of 1933.3. The root-mean-square deviation (RMSD) is 0.308 Å for 312 pruned atom pairs and 10.208 Å across all 388 pairs, indicating a mismatch in the unstructured C-terminal loops that fail to align (asterisk). In contrast, the surface-exposed β-sheet regions are almost identical, except for the Liprin-1 peptide helix (black arrows).

Fig. 2 Arthritis induction with LIP1 peptide

(A) Outline of the experimental design. 8 weeks-old mice received on day 0 and boosted on day 21 intradermally at the basis of the tail 200 µg of collagen an Liprin-1 peptide both with Complete Freund's adjuvant (CFA). The animals (n=10 for each group) were sacrificed 60 days after CIA and LIA induction.

(B) *Left part:* comparison of arthritic score of non-treated mice (sham), Collagen-induced (CIA) and Liprin-1peptide induced (LIA) mice. Clinical parameters such as slight edema and erythema limited to ankle, slight edema and erythema from the ankle to the tarsal bone, moderate edema and erythema the ankle to the tarsal bone, edema and erythema from the ankle to the entire leg have been considered for clinical score. Statistical significance was determined by 1-way ANOVA: ####: $p<0.001$ in comparison with the sham group. *Right part:* corresponding cumulative score.

(C) Comparison of histological score of non-treated mice (sham), CIA and LIA mice. Statistical significance was determined by 1-way ANOVA: ***: $p<0.005$; ns: not significant. After 60 days, ankle-joints were evaluated by addressing clinical score from 1 to 4: (1) slight edema and erythema limited to ankle; (2) slight edema and erythema from the ankle to the tarsal bone; (3) moderate edema and erythema the ankle to the tarsal bone; (4): edema and erythema from the ankle to the entire leg.

(D) Representative imagines of histological sections of ankle-joints of analyzed animal groups.

(E) Effect on pro-inflammatory cytokines profiles (MCP-1, IL-1β, IL-6, IL-12p70, IL-17A, INF-γ, TNF-α,) in sera of treated animals. Statistical significance was determined by 1-way ANOVA: *: $p<0.05$; ***: $p<0.005$; ****: $p<0.001$; ns: not significant.

(F) Percentage of CD4+CD25+FoxP3+ Treg cells among CD4+ cells in splenocytes of mice analyzed by flow cytometric analysis. Statistical significance was determined by 1-way ANOVA: **: $p<0.01$; ns: not significant.

Fig. 3 Impact of the route of administration on TBSV.pLip-mediated tolerance induction

(A) Outline of the experimental design. 8 weeks-old mice received on day 0 and boosted on day 21 intradermally at the basis of the tail 200 µg of collagen with Complete Freund's adjuvant (CFA). The animals (n=10 for each group) were divided into 7 groups on day 28 based on clinical score and/or paw volume. 7 doses of 50µg of TBSV.pLip were administered by different injection routes: intra-peritoneal (i.p.), intra-venous (i.v.), sub-cutaneous (s.c.) and oral (p.o.); control groups were: untreated mice (CIA), sham group and a group receiving dexamethasone (1 mg/kg) every other day (Dexa). The animals were sacrificed 60 days after CIA induction.

(B) *Left part:* Comparison of clinical score of all the animal groups. Clinical parameters such as slight edema and erythema limited to ankle, slight edema and erythema from the ankle to the tarsal bone, moderate edema and erythema the ankle to the tarsal bone, edema and erythema from the ankle to the entire leg have been considered for clinical score. Statistical significance was determined by 1-way ANOVA. *: $p<0.05$, **: $p<0.01$, ****: $p<0.001$ in comparison with the CIA group; ####: $p<0.001$ in comparison with the sham group, ns: not significant. *Right part:* corresponding cumulative scores.

(C) Comparison of histological score in ankle-joints of analyzed animal groups. Statistical significance was determined by 1-way ANOVA: *: $p<0.05$; ****: $p<0.001$; ns: not significant in comparison with CIA. After 60 days, ankle-joints were evaluated by addressing clinical score from 1 to 4: (1) slight edema and erythema limited to ankle; (2) slight edema and erythema from the ankle to the tarsal bone; (3) moderate edema and erythema the ankle to the tarsal bone; (4): edema and erythema from the ankle to the entire leg.

(D) Representative images of histological sections of ankle-joints of analyzed animal groups.

(E) Pro-inflammatory cytokines profiles (MCP-1, IL-1β, IL-6, IL-12p70, IL-17A, INF-γ, TNF-α,) in sera of analyzed mice. Statistical significance was assessed by 1-way ANOVA: *: $p<0.05$, **: $p<0.01$; ***: $p<0.005$; ****: $p<0.001$ in comparison to CIA.

(F) Percentage of CD4+CD25+FoxP3+ Treg cells among CD4+ cells in splenocytes of mice analyzed by flow cytometric analysis. Statistical significance was determined by 1-way ANOVA: *: $p<0.05$, **: $p<0.01$; ***: $p<0.005$; ****: $p<0.001$ in comparison to CIA.

Fig. 4 Impact of different dose numbers on TBSV.pLip mediated tolerance

(A) Outline of the experimental design. 8 weeks-old mice received on day 0 and boosted on day 21 intradermally at the basis of the tail 200 µg of collagen with Complete Freund's adjuvant (CFA). The animals (n=10 for each group) were divided into 7 groups on day 28 based on clinical score and/or paw volume. 50µg of TBSV.pLip were administered i.v. either 7-, 4- ,2- or 1-time i.v. on different days as specified. Control groups included untreated mice (CIA), sham group and a group receiving dexamethasone (1 mg/kg) every other day (dexa). The animals were sacrificed 60 days after CIA induction.

(B) *Left part*: Comparison of clinical score of non-treated mice (sham), saline-treated CIA mice (CIA), Dexamethasone-treated CIA mice and mice treated by intravenous administrations of 7, 4, 2 and 1

i.v. doses of TBSV.pLip (50 µg). Clinical parameters such as slight edema and erythema limited to ankle, slight edema and erythema from the ankle to the tarsal bone, moderate edema and erythema the ankle to the tarsal bone, edema and erythema from the ankle to the entire leg have been considered for clinical score. Statistical significance was determined by 1-way ANOVA: **: $p<0.01$, ****: $p<0.001$ in comparison with the CIA group; ####: $p<0.001$ in comparison with the sham group. *Right part:* corresponding cumulative scores.

(C) Comparison of histological score in ankle-joints of analyzed animal groups. Statistical significance was determined by 1-way ANOVA: **: $p<0.01$, ****: $p<0.001$, ns: not significant, compared with the CIA group. After 58 days, ankle-joints were evaluated by addressing clinical score from 1 to 4: (1) slight edema and erythema limited to ankle; (2) slight edema and erythema from the ankle to the tarsal bone; (3) moderate edema and erythema the ankle to the tarsal bone; (4): edema and erythema from the ankle to the entire leg.

(D) Representative imagines of histological sections of ankle-joints of analyzed animal groups.

(E) Pro-inflammatory cytokines profiles (MCP-1, IL-1β, IL-6, IL-12p70, IL-17A, INF-γ, TNF-α,) in sera of analyzed mice. Statistical significance was assessed by 1-way ANOVA: *: $p<0.05$, **: $p<0.01$; ***: $p<0.005$; ****: $p<0.001$.

(F) Percentage of CD4+CD25+FoxP3+ Treg cells among CD4+ cells in splenocytes of analyzed mice. Statistical significance was determined by 1-way ANOVA: **: $p<0.01$, ****: $p<0.001$, ns: not significant.

Fig. 5 Dose-Effect of TBSV.pLip mediated tolerance

(A) Outline of the experimental design. 8 weeks-old mice received on day 0 and boosted on day 21 intradermally at the basis of the tail 200 µg of collagen with Complete Freund's adjuvant (CFA). The animals (n=20 for each group) were divided into 7 groups on day 28 based on clinical score and/or paw volume. 5, 20, 50 and 200 µg of TBSV.pLip were administered i.v. 4 times. Control groups included untreated mice (CIA), sham group and a group receiving dexamethasone (1 mg/kg) every other day (Dexa). The animals were sacrificed 70 days after CIA induction. CIA, 3 animals per Sham and TBSV.pLip treated animals were sacrificed for blood collection at days 37, 47 and 57 after CIA induction.

(B) *Left part*: Comparison of clinical score of non-treated mice (sham), saline-treated CIA mice (CIA), Dexamethasone-treated CIA mice and mice treated by 4 i.v. administrations of 200, 50, 20, 5 µg of TBSV.pLip. Clinical parameters such as slight edema and erythema limited to ankle, slight edema and erythema from the ankle to the tarsal bone, moderate edema and erythema the ankle to the tarsal bone, edema and erythema from the ankle to the entire leg have been considered for clinical score. Statistical significance was determined by 1-way ANOVA: *: $p<0.05$, ****: $p<0.001$, ns: not significant in comparison with the CIA group; ####: $p<0.001$ in comparison with the sham group. *Right part:* corresponding cumulative scores.

(C) Comparison of histological score in ankle-joints of analyzed animal groups. Statistical significance was determined by 1-way ANOVA: *: $p<0.05$, ***: $p<0.005$, ****: $p<0.001$, ns: not significant.

(D) Representative imagines of histological sections of ankle-joints of analyzed animal groups.

(E) Pro-inflammatory cytokines profiles (MCP-1, IL-1β, IL-6, IL-12p70, IL-17A, INF-γ, TNF-α,) in sera of analyzed mice. Statistical significance was determined by 1-way ANOVA: *: $p<0.05$, **: $p<0.01$; ***: $p<0.005$; ****: $p<0.001$.

(F) Percentage of CD4+CD25+FoxP3+ Treg cells among CD4+ cells in splenocytes of analyzed mice. Statistical significance was determined by 1-way ANOVA: *: $p<0.05$, **: $p<0.01$; ***: $p<0.005$; ****: $p<0.001$.

Fig. 6 Role of the spleen on the tolerance induction mediated by TBSV.pLip

(A) Outline of the experimental design. 8 weeks-old mice received on day 0 and boosted on day 21 intradermally at the basis of the tail 200 µg of collagen with Complete Freund's adjuvant (CFA). The animals (n=10 for each group) were divided into 6 groups on day 28 based on clinical score and/or paw volume. 50 µg of TBSV.pLip were administered i.v. 4 times to CIA mice either splenectomized and not. Control groups included untreated mice (CIA) either splenectomized and not, sham group and a group receiving dexamethasone (1 mg/kg) every other day (Dexa). The animals were sacrificed 60 days after CIA induction.

(B) *Left part:* Comparison in arthritic score of mice either exposed or not to splenectomy treated by 4 i.v. doses of 50 µg TBSV.pLip and non-treated mice (sham). Clinical parameters such as slight edema and erythema limited to ankle, slight edema and erythema from the ankle to the tarsal bone, moderate edema and erythema the ankle to the tarsal bone, edema and erythema from the ankle to the entire leg have been considered for clinical score. Statistical significance was determined by 1-way ANOVA: *: $p<0.05$, ****: $p<0.001$, ns: not significant in comparison with the CIA group; ####: $p<0.001$ in comparison with the sham group. *Right part:* corresponding cumulative scores.

(C) Comparison of histological score in ankle-joints of analyzed animal groups. Statistical significance was determined by 1-way ANOVA: *: $p<0.05$, **: $p<0.01$; ***: $p<0.005$; ****: $p<0.001$ in comparison to CIA Spleen+.

(D) Representative imagines of histological sections of ankle-joints of analyzed animal groups.

(E) Pro-inflammatory cytokines profiles (MCP-1, IL-1β, IL-6, IL-12p70, IL-17A, INF-γ, TNF-α,) in sera of analyzed mice. Statistical significance was determined by 1-way ANOVA: *: $p<0.05$, **: $p<0.01$; ***: $p<0.005$; ****: $p<0.001$.

(F) Total IgG in treated mice against the Liprin-1 peptide evaluated by ELISA (n=3 for each group). Statistical significance was determined by 1-way ANOVA: *: $p<0.05$, **: $p<0.01$; ***: $p<0.005$; ****: $p<0.001$. n.s.: non-significant.

Fig. 7 Impact of the viral shell on tolerance induction

(A) Outline of the experimental design. 8 weeks-old mice received on day 0 and boosted on day 21 intradermally at the basis of the tail 200 µg of collagen with Complete Freund's adjuvant (CFA). The animals (n=10 for each group) were divided into 4 groups on day 28 based on clinical score and/or paw volume. 50 µg of either TBSV.pLip and TBSV WT were administered i.v. 4 times. Control groups included untreated mice (CIA), sham group and a group receiving dexamethasone (1 mg/kg) every other day (Dexa). The animals were sacrificed 60 days after CIA induction.

(B) *Left part*: Comparison of clinical score of non-treated mice (sham), saline-treated CIA mice (CIA), Dexamethasone-treated CIA mice and mice treated by 4 intravenous administrations of 50µg of TBSV.pLip and of TBSV WT. Clinical parameters such as slight edema and erythema limited to ankle, slight edema and erythema from the ankle to the tarsal bone, moderate edema and erythema the ankle to the tarsal bone, edema and erythema from the ankle to the entire leg have been considered for clinical score. Statistical significance was determined by 1-way ANOVA: *: $p<0.05$, ****:

p<0.001, ns: not significant in comparison with the CIA group; ####: p<0.001 in comparison with the sham group. *Right part:* corresponding cumulative scores.

(C) Comparison of histological score in ankle-joints of analyzed animal groups. Statistical significance was determined by 1-way ANOVA: *: p<0.05, **: p<0.01; ***: p<0.005; ****: p<0.001.

(D) Representative imagines of histological sections of ankle-joints of analyzed animal groups.

(E) Pro-inflammatory cytokines profiles (MCP-1, IL-1β, IL-6, IL-12p70, IL-17A, INF-γ, TNF-α,) in sera of analyzed mice. Statistical significance was determined by 1-way ANOVA: *: p<0.05, **: p<0.01; ***: p<0.005; ****: p<0.001.

(F) Anti-inflammatory cytokines profiles (IL-4, IL-10 and TGF-β) in sera of analyzed mice. Statistical significance was determined by 1-way ANOVA: *: p<0.05, **: p<0.01; ***: p<0.005; ****: p<0.001.

(G) Percentage of CD4+CD25+FoxP3+ Treg cells among CD4+ cells in splenocytes of analyzed mice. Statistical significance was determined by 1-way ANOVA: *: p<0.05, **: p<0.01; ***: p<0.005; ****: p<0.001.

(H) Immunofluorescence co-labeling analysis of tolerogenic dendritic cells ($CD11c^+/PD\text{-}L1^+$) in the mesenteric lymph nodes across the experimental groups. *: p<0.05, **: p<0.01; ***: p<0.005; ****: p<0.001.

(I) Total IgG in treated mice against the Liprin-1 peptide evaluated by ELISA (n=3 for each group). Statistical significance was determined by 1-way ANOVA: *: p<0.05, **: p<0.01; ***: p<0.005; ****: p<0.001. n.s.: non-significant.

List of Supplementary Materials

Table S1: Data file reporting all the statistical analysis performed for all pre-clinical experiments reported.

Figure S2: Biodistribution of TBSV.pLip following intravenous administration.

Tissue uptake is expressed as percentage of injected dose per gram of tissue (%ID/g) in major organs (liver, spleen, kidney, stomach, heart, lungs, and brain). Purple bars represent TBSV.pLip 4 intravenous injections (4 i.v.), while green bars represent 7 intravenous injections (7 i.v.). Data are shown as mean ± standard deviation. In purple: 7 i.v. injections of TBSV.pLip, in green: 4 i.v. injections of TBSV.pLip.

Figure S3: Comparative Analysis of Viral Shell Immunomodulation via TBSV WT and TBSV.pLip 7 i.v. Injections

The outline of the experiment is the same as the one reported in Figure 3A.

(A) *Left part*: Comparison of clinical score of non-treated mice (sham), saline-treated CIA mice (CIA), Dexamethasone-treated CIA mice and mice treated by 7 intravenous administrations of 50µg of TBSV.pLip and of TBSV WT. Clinical parameters such as slight edema and erythema limited to ankle, slight edema and erythema from the ankle to the tarsal bone, moderate edema and erythema the ankle to the tarsal bone, edema and erythema from the ankle to the entire leg have been

considered for clinical score. Statistical significance was determined by 1-way ANOVA: *: $p<0.05$, ****: $p<0.001$, ns: not significant in comparison with the CIA group; ####: $p<0.001$ in comparison with the sham group. *Right part:* corresponding cumulative score.

(B) Comparison of histological score in ankle-joints of analyzed animal groups. Statistical significance was determined by 1-way ANOVA: *: $p<0.05$, **: $p<0.01$; ***: $p<0.005$; ****: $p<0.001$.

(C) Representative imagines of histological sections of ankle-joints of analyzed animal groups.

(D) Pro-inflammatory cytokines profiles (MCP-1, IL-1β, IL-6, IL-12p70, IL-17A, INF-γ, TNF-α,) in sera of analyzed mice. Statistical significance was determined by 1-way ANOVA: *: $p<0.05$, **: $p<0.01$; ***: $p<0.005$; ****: $p<0.001$.

(E) Percentage of CD4+CD25+FoxP3+ Treg cells among CD4+ cells in splenocytes of analyzed mice. Statistical significance was determined by 1-way ANOVA: *: $p<0.05$, **: $p<0.01$; ***: $p<0.005$; ****: $p<0.001$.

Figure S4: Assessment of combined i.v. and s.c. administrations of TBSV.pLip for Tolerance Induction

(A) Outline of the experimental design. 8 weeks-old mice received on day 0 and boosted on day 21 intradermally at the basis of the tail 200 µg of collagen with Complete Freund's adjuvant (CFA). The animals (n=10 for each group) were divided into 4 groups on day 28 based on clinical score and/or paw volume. 50 µg of TBSV.pLip were administered i.v. and/or s.c. as indicated. Control groups included untreated mice (CIA), sham group and a group receiving dexamethasone (1 mg/kg) every other day (Dexa). The animals were sacrificed 60 days after CIA induction.

(B) *Left part*: Comparison of clinical score of non-treated mice (sham), saline-treated CIA mice (CIA), Dexamethasone-treated CIA mice and mice treated by sub-cutaneous and/or intravenous administrations of 50µg of TBSV.pLip. Clinical parameters such as slight edema and erythema limited to ankle, slight edema and erythema from the ankle to the tarsal bone, moderate edema and erythema the ankle to the tarsal bone, edema and erythema from the ankle to the entire leg have been considered for clinical score. Statistical significance was determined by 1-way ANOVA: *: $p<0.05$, ****: $p<0.001$, ns: not significant in comparison with the CIA group; ####: $p<0.001$ in comparison with the sham group. *Right part:* corresponding cumulative score.

(C) Comparison of histological score in ankle-joints of analyzed animal groups. Statistical significance was determined by 1-way ANOVA: *: $p<0.05$, **: $p<0.01$; ***: $p<0.005$; ****: $p<0.001$.

(D) Representative imagines of histological sections of ankle-joints of analyzed animal groups.

(E) Pro-inflammatory cytokines profiles (MCP-1, IL-1β, IL-6, IL-12p70, IL-17A, INF-γ, TNF-α,) in sera of analyzed mice. Statistical significance was determined by 1-way ANOVA: *: $p<0.05$, **: $p<0.01$; ***: $p<0.005$; ****: $p<0.001$.

(F) Percentage of CD4+CD25+FoxP3+ Treg cells among CD4+ cells in splenocytes of analyzed mice. Statistical significance was determined by 1-way ANOVA: *: $p<0.05$, **: $p<0.01$; ***: $p<0.005$; ****: $p<0.001$.

Figure S5: Tolerance induction in LIA mice by TBSV.pLip

(A) Outline of the experimental design. 8 weeks-old mice received on day 0 and boosted on day 21 intradermally at the basis of the tail 200 µg of Liprin-1 peptide with Complete Freund's adjuvant (CFA). The animals (n=10 for each group) were divided into 4 groups on day 28 based on clinical score and/or paw volume. 50 µg of TBSV.pLip were administered i.v. Control group of untreated mice (sham group). The animals were sacrificed 60 days after LIA induction.

(B) *Left part*: Comparison of clinical score of non-treated mice (sham), Liprin-1 peptide-treated mice (LIA) and mice treated by intravenous administrations of 50µg of TBSV.pLip. Clinical parameters such as slight edema and erythema limited to ankle, slight edema and erythema from the ankle to the tarsal bone, moderate edema and erythema the ankle to the tarsal bone, edema and erythema from the ankle to the entire leg have been considered for clinical score. Statistical significance was determined by 1-way ANOVA: *: $p<0.05$, ****: $p<0.001$, ns: not significant in comparison with the CIA group; ####: $p<0.001$ in comparison with the sham group. *Right part:* corresponding cumulative scores.

(C) Comparison of histological score in ankle-joints of analyzed animal groups. Statistical significance was determined by 1-way ANOVA: *: $p<0.05$, **: $p<0.01$; ***: $p<0.005$; ****: $p<0.001$.

(D) Representative imagines of histological sections of ankle-joints of analyzed animal groups.

(E) Pro-inflammatory cytokines profiles (MCP-1, IL-1β, IL-6, IL-12p70, IL-17A, INF-γ, TNF-α,) in sera of analyzed mice. Statistical significance was determined by 1-way ANOVA: *: $p<0.05$, **: $p<0.01$; ***: $p<0.005$; ****: $p<0.001$.

(F) Percentage of CD4+CD25+FoxP3+ Treg cells among CD4+ cells in splenocytes of analyzed mice. Statistical significance was determined by 1-way ANOVA: *: $p<0.05$, **: $p<0.01$; ***: $p<0.005$; ****: $p<0.001$.

References and Notes

1. Weyand, C. M. & Goronzy, J. J. The immunology of rheumatoid arthritis. *Nat. Immunol.* **22**, 10–18 (2021).
2. Black, R. J. *et al.* Global, regional, and national burden of rheumatoid arthritis, 1990–2020, and projections to 2050: a systematic analysis of the Global Burden of Disease Study 2021. *Lancet Rheumatol.* **5**, e594–e610 (2023).
3. Shuai, Z. *et al.* Reestablish immune tolerance in rheumatoid arthritis. *Front. Immunol.* **13**, 1012868 (2022).
4. Willyard, C. Can autoimmune diseases be cured? Scientists see hope at last. *Nature* **625**, 646–648 (2024).

5. Cifuentes-Rius, A., Desai, A., Yuen, D., Johnston, A. P. R. & Voelcker, N. H. Inducing immune tolerance with dendritic cell-targeting nanomedicines. *Nat. Nanotechnol.* **16**, 37–46 (2021).

6. Serra, P. & Santamaria, P. Nanoparticle-based autoimmune disease therapy. *Clin. Immunol.* **160**, 3–13 (2015).

7. Montaño, J., Garnica, J. & Santamaria, P. Immunomodulatory and immunoregulatory nanomedicines for autoimmunity. *Semin. Immunol.* **56**, 101535 (2021).

8. Serra, P. & Santamaria, P. Antigen-specific therapeutic approaches for autoimmunity. *Nat. Biotechnol.* **37**, 238–251 (2019).

9. Zampieri, R. *et al.* Prevention and treatment of autoimmune diseases with plant virus nanoparticles. *Sci. Adv.* **6**, eaaz0295 (2020).

10. Benvenuto, E. *et al.* Plant molecular farming in the wake of the closure of Medicago Inc. *Nat. Biotechnol.* **41**, 893–894 (2023).

11. Pivotto D, Rosa A, Gecchele E, Zampieri R, Raneri A, Elsheikh AM, Garonzi V and Avesani L (2026) Clinical-grade plant-made nanomaterials: from process design to the construction of a manufacturing facility. Front. Plant Sci. 16:1724810. doi: 10.3389/fpls.2025.1724810

12. Malyala, P. & Singh, M. Endotoxin Limits in Formulations for Preclinical Research. *J. Pharm. Sci.* **97**, 2041–2044 (2008).

13. Bason, C. *et al.* Identification of a Novel Serological Marker in Seronegative Rheumatoid Arthritis Using the Peptide Library Approach. *Front. Immunol.* **12**, 753400 (2021).

14. Batsalova, T., Lindh, I., Bäcklund, J., Dzhambazov, B. & Holmdahl, R. Comparative analysis of collagen type II-specific immune responses during development of collagen-induced arthritis in two B10 mouse strains. *Arthritis Res. Ther.* **14**, R237 (2012).

15. Serra, P. & Santamaria, P. Antigen-specific therapeutic approaches for autoimmunity. *Nat. Biotechnol.* **37**, 238–251 (2019).

16. Li, S. C., Rangel, A. D. & Kabeer, M. H. Precision Technique for Splenectomy Limits Mouse Stress Responses for Accurate and Realistic Measurements for Investigating Inflammation and Immunity. *Bio-Protoc.* **9**, e3317 (2019).

17. Huang, J. *et al.* Promising Therapeutic Targets for Treatment of Rheumatoid Arthritis. *Front. Immunol.* **12**, 686155 (2021).

18. Varshney, P. *et al.* A randomized controlled study of peanut oral immunotherapy: Clinical desensitization and modulation of the allergic response. *J. Allergy Clin. Immunol.* **127**, 654–660 (2011).

19. Zimmerman, D. H. *et al.* Current status of immunological therapies for rheumatoid arthritis with a focus on antigen-specific therapeutic vaccines. *Front. Immunol.* **15**, 1334281 (2024).

20. Thorp, E. B., Boada, C., Jarbath, C. & Luo, X. Nanoparticle Platforms for Antigen-Specific Immune Tolerance. *Front. Immunol.* **11**, 945 (2020).

21. Bruns, L. *et al.* Immunization with an immunodominant self-peptide derived from glucose-6-phosphate isomerase induces arthritis in DBA/1 mice. *Arthritis Res. Ther.* **11**, R117 (2009).

22. Hunter, Z. *et al.* A Biodegradable Nanoparticle Platform for the Induction of Antigen-Specific Immune Tolerance for Treatment of Autoimmune Disease. *ACS Nano* **8**, 2148–2160 (2014).

23. Kuo, R., Saito, E., Miller, S. D. & Shea, L. D. Peptide-Conjugated Nanoparticles Reduce Positive Co-stimulatory Expression and T Cell Activity to Induce Tolerance. *Mol. Ther.* **25**, 1676–1685 (2017).

24. Carambia, A. *et al.* Nanoparticle-based autoantigen delivery to Treg-inducing liver sinusoidal endothelial cells enables control of autoimmunity in mice. *J. Hepatol.* **62**, 1349–1356 (2015).

25. Saito, E. *et al.* Design of biodegradable nanoparticles to modulate phenotypes of antigen-presenting cells for antigen-specific treatment of autoimmune disease. *Biomaterials* **222**, 119432 (2019).

26. Clemente-Casares, X. *et al.* Expanding antigen-specific regulatory networks to treat autoimmunity. *Nature* **530**, 434–440 (2016).

27. Singha, S. *et al.* Peptide–MHC-based nanomedicines for autoimmunity function as T-cell receptor microclustering devices. *Nat. Nanotechnol.* **12**, 701–710 (2017).

28. Li, H., Zhang, G. X. & Rostami, A. CD11c+CD11b+ dendritic cells play an important role in intravenous tolerance and suppress ongoing experimental autoimmune encephalomyelitis. *FASEB J.* **22**, (2008).

29. Burton, B. R. *et al.* Sequential transcriptional changes dictate safe and effective antigen-specific immunotherapy. *Nat. Commun.* **5**, 4741 (2014).

30. Larché, M. & Wraith, D. C. Peptide-based therapeutic vaccines for allergic and autoimmune diseases. *Nat. Med.* **11**, S69–S76 (2005).

31. Ackun-Farmmer, M. & Jewell, C. M. Enhancing the functionality of self-assembled immune signals using chemical crosslinks. *Front. Immunol.* **14**, 1079910 (2023).

32. Getts, D. R. *et al.* Tolerance Induced by Apoptotic Antigen-Coupled Leukocytes Is Induced by PD-L1+ and IL-10–Producing Splenic Macrophages and Maintained by T Regulatory Cells. *J. Immunol.* **187**, 2405–2417 (2011).

33. Lico, C. *et al.* A biodistribution study of two differently shaped plant virus nanoparticles reveals new peculiar traits. *Colloids Surf. B Biointerfaces* **148**, 431–439 (2016).

34. Zheng, W. *et al.* Role of Kupffer cells in tolerance induction after liver transplantation. *Front. Cell Dev. Biol.* **11**, 1179077 (2023).

35. Lüth, S. *et al.* Ectopic expression of neural autoantigen in mouse liver suppresses experimental autoimmune neuroinflammation by inducing antigen-specific Tregs. *J. Clin. Invest.* JCI32132 (2008) doi:10.1172/JCI32132.

36. Tiegs, G. & Lohse, A. W. Immune tolerance: What is unique about the liver. *J. Autoimmun.* **34**, 1–6 (2010).

37. Larmonier, N. *et al.* Tumor-derived CD4(+)CD25(+) regulatory T cell suppression of dendritic cell function involves TGF-beta and IL-10. *Cancer Immunol. Immunother. CII* **56**, 48–59 (2007).

38. Yang, W.-C. *et al.* Interleukin-4 Supports the Suppressive Immune Responses Elicited by Regulatory T Cells. *Front. Immunol.* **8**, 1508 (2017).

39. Oldfield, W. L. G., Kay, A. B. & Larché, M. Allergen-Derived T Cell Peptide-Induced Late Asthmatic Reactions Precede the Induction of Antigen-Specific Hyporesponsiveness in Atopic Allergic Asthmatic Subjects. *J. Immunol.* **167**, 1734–1739 (2001).

40. Abramson, J. *et al.* Accurate structure prediction of biomolecular interactions with AlphaFold 3. *Nature* **630**, 493–500 (2024).

41. Pettersen, E. F. *et al.* UCSF CHIMERAX : Structure visualization for researchers, educators, and developers. *Protein Sci.* **30**, 70–82 (2021).

42. Stevanin, M. *et al.* CD11b regulates the Treg/Th17 balance in murine arthritis via IL-6. *Eur. J. Immunol.* **47**, 637–645 (2017).

43. Mahmoud, A. M. *et al.* Disclosing the impact of metformin and methotrexate in adjuvant arthritis in female rats: molecular docking and biochemical insights on visfatin. *Naunyn. Schmiedebergs Arch. Pharmacol.* **398**, 8923–8934 (2025).

44. Zhang, Y., Wang, S., Song, S., Yang, X. & Jin, G. Ginsenoside Rg3 Alleviates Complete Freund's Adjuvant-Induced Rheumatoid Arthritis in Mice by Regulating CD4+CD25+Foxp3+Treg Cells. *J. Agric. Food Chem.* **68**, 4893–4902 (2020).

45. Li, S. C., Rangel, A. D. & Kabeer, M. H. Precision Technique for Splenectomy Limits Mouse Stress Responses for Accurate and Realistic Measurements for Investigating Inflammation and Immunity. *Bio-Protoc.* **9**, e3317 (2019).

ACKNOWLEDGMENTS:

Authors acknowledge CPT (Centro Piattaforme Tecnologiche) of the University of Verona for the access and support to the DLS equipment.

FUNDING:

This work has been co-funded by the EIC 2024 Accelerator program, specifically through the“Diamante” project under grant agreement number 101189019. Part of the work has been supported by ‘Finanziamento dell’Unione Europea-Next Generation EU, Missione 4, Componente 1 CUP B53D23024740001’

AUTHOR CONTRIBUTIONS:

COMPETING INTERESTS:

LA and RZ were founders of Dimante SB srl. AR, EG and RZ are employees of Diamante SB srl. The work here described has been patented.
AM, JM, JB, NS and SF are part of the scientific advisory board of Diamante SB srl.
The remaining author(s) declared that this work was conducted in the absence of any commercial or financial relationships that could be construed as a potential conflict of interest.

DATA AND MATERIAL AVAILABILITY:
All raw data relative to the experiemnts reported are present in Table 1 of the Supplementary Materials

Figure 1

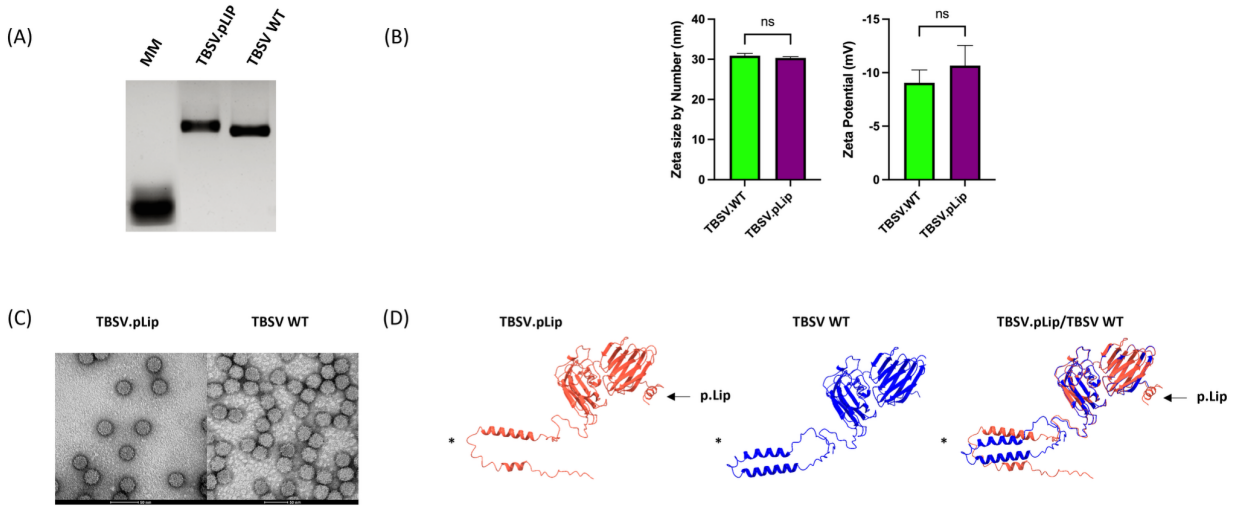
(A)
MM
TBSV.pLIP
TBSV WT
(B)
Zeta size by Number (nm)
ns
TBSV.WT
TBSV.pLip
Zeta Potential (mV)
ns
TBSV.WT
TBSV.pLip
(C)
TBSV.pLip
TBSV WT
(D)
TBSV.pLip
p.Lip
TBSV WT
TBSV.pLip/TBSV WT
p.Lip

Figure 2

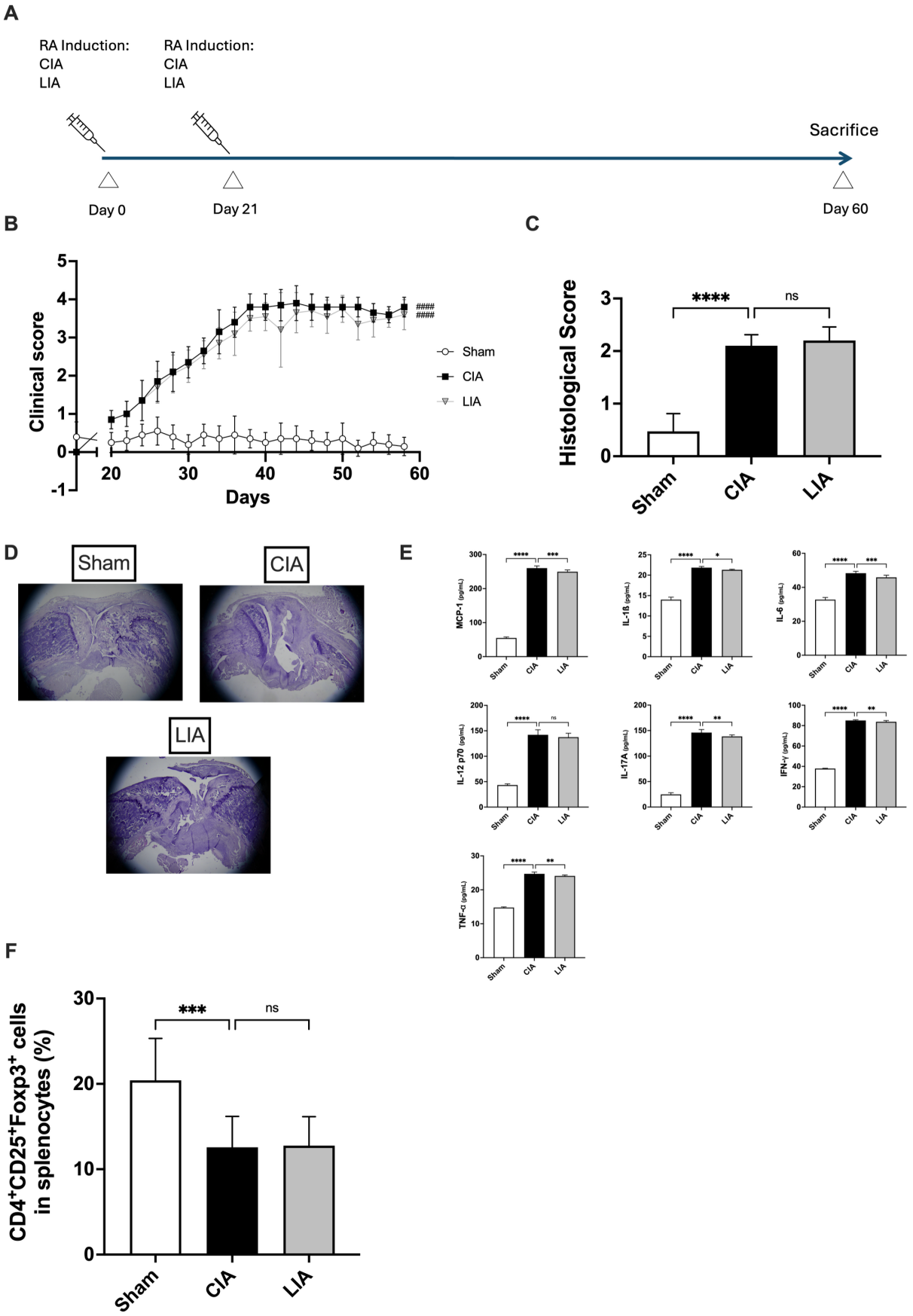
A
RA Induction:
CIA
LIA
RA Induction:
CIA
LIA
Sacrifice
Day 0
Day 21
Day 60
B
Clinical score
Days
Sham
CIA
LIA
C
Histological Score
****
ns
Sham
CIA
LIA
D
Sham
CIA
LIA
E
MCP-1 (pg/mL)
IL-1β (pg/mL)
IL-6 (pg/mL)
IL-12 p70 (pg/mL)
IL-17A (pg/mL)
IFN-γ (pg/mL)
TNF-α (pg/mL)
F
CD4+CD25+Foxp3+ cells in splenocytes (%)
***
ns
Sham
CIA
LIA

Figure 3

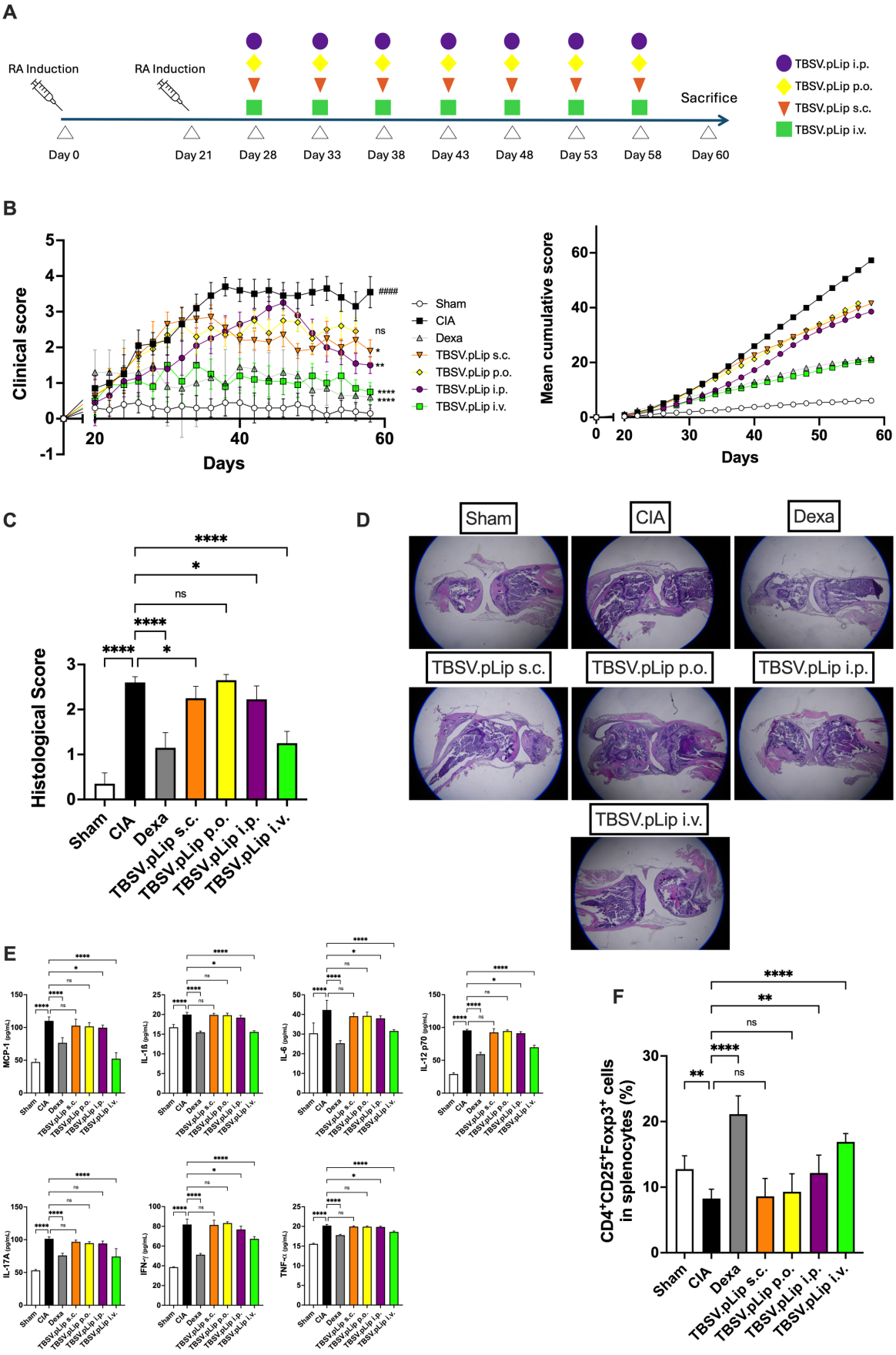
A
RA Induction
RA Induction
Sacrifice
Day 0
Day 21
Day 28
Day 33
Day 38
Day 43
Day 48
Day 53
Day 58
Day 60
TBSV.pLip i.p.
TBSV.pLip p.o.
TBSV.pLip s.c.
TBSV.pLip i.v.
B
Clinical score
Days
Sham
CIA
Dexa
TBSV.pLip s.c.
TBSV.pLip p.o.
TBSV.pLip i.p.
TBSV.pLip i.v.
Mean cumulative score
Days
C
Histological Score
Sham
CIA
Dexa
TBSV.pLip s.c.
TBSV.pLip p.o.
TBSV.pLip i.p.
TBSV.pLip i.v.
D
Sham
CIA
Dexa
TBSV.pLip s.c.
TBSV.pLip p.o.
TBSV.pLip i.p.
TBSV.pLip i.v.
E
MCP-1 (pg/mL)
IL-1β (pg/mL)
IL-6 (pg/mL)
IL-12 p70 (pg/mL)
IL-17A (pg/mL)
IFN-γ (pg/mL)
TNF-α (pg/mL)
F
CD4+CD25+Foxp3+ cells in splenocytes (%)
Sham
CIA
Dexa
TBSV.pLip s.c.
TBSV.pLip p.o.
TBSV.pLip i.p.
TBSV.pLip i.v.

Figure 4

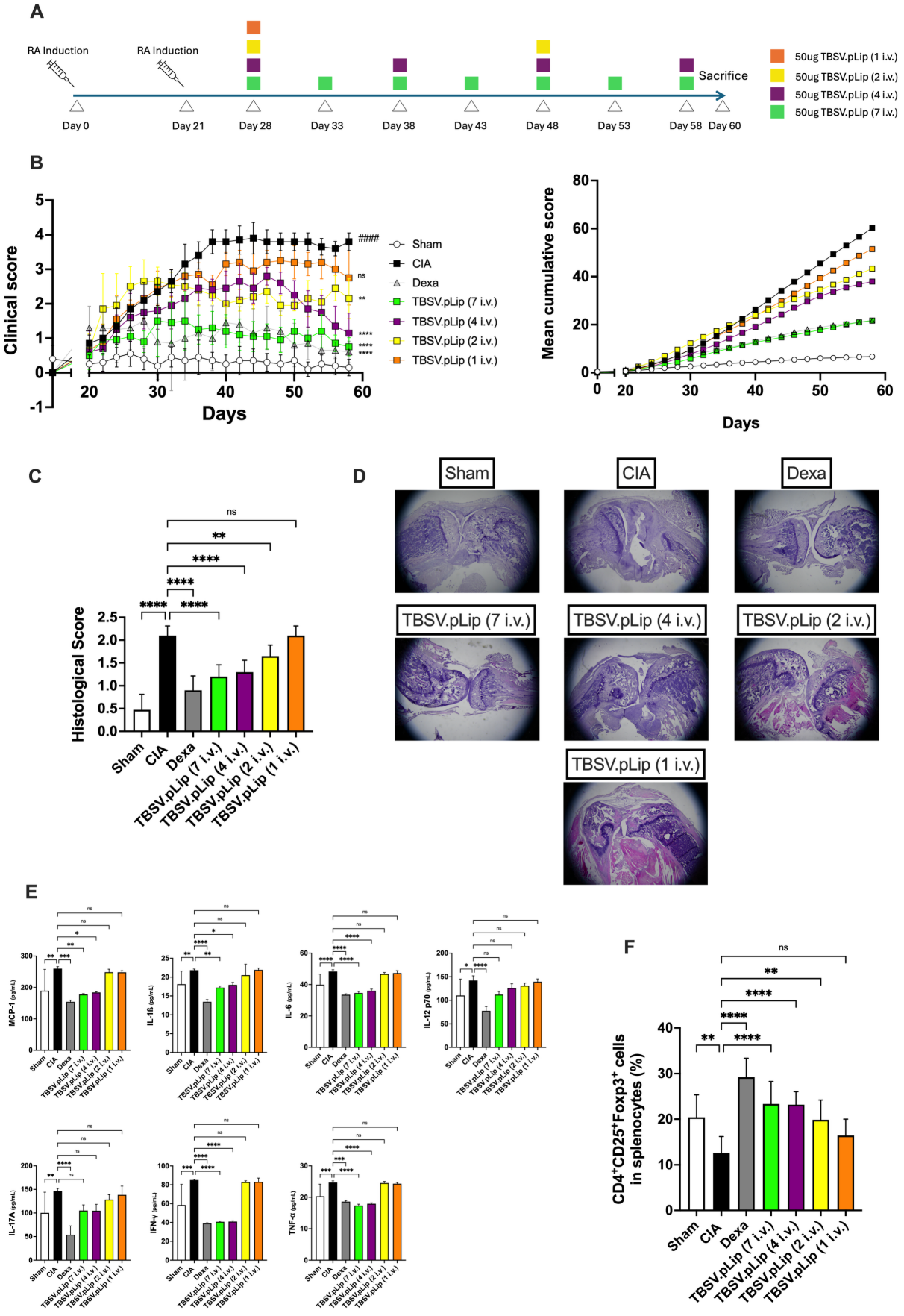
A
RA Induction
RA Induction
Sacrifice
Day 0
Day 21
Day 28
Day 33
Day 38
Day 43
Day 48
Day 53
Day 58
Day 60
50ug TBSV.pLip (1 i.v.)
50ug TBSV.pLip (2 i.v.)
50ug TBSV.pLip (4 i.v.)
50ug TBSV.pLip (7 i.v.)
B
Clinical score
Days
Sham
CIA
Dexa
TBSV.pLip (7 i.v.)
TBSV.pLip (4 i.v.)
TBSV.pLip (2 i.v.)
TBSV.pLip (1 i.v.)
Mean cumulative score
Days
C
Histological Score
Sham
CIA
Dexa
TBSV.pLip (7 i.v.)
TBSV.pLip (4 i.v.)
TBSV.pLip (2 i.v.)
TBSV.pLip (1 i.v.)
D
Sham
CIA
Dexa
TBSV.pLip (7 i.v.)
TBSV.pLip (4 i.v.)
TBSV.pLip (2 i.v.)
TBSV.pLip (1 i.v.)
E
MCP-1 (pg/mL)
IL-1β (pg/mL)
IL-6 (pg/mL)
IL-12 p70 (pg/mL)
IL-17A (pg/mL)
IFN-γ (pg/mL)
TNF-α (pg/mL)
F
CD4+CD25+Foxp3+ cells in splenocytes (%)
Sham
CIA
Dexa
TBSV.pLip (7 i.v.)
TBSV.pLip (4 i.v.)
TBSV.pLip (2 i.v.)
TBSV.pLip (1 i.v.)

Figure 5

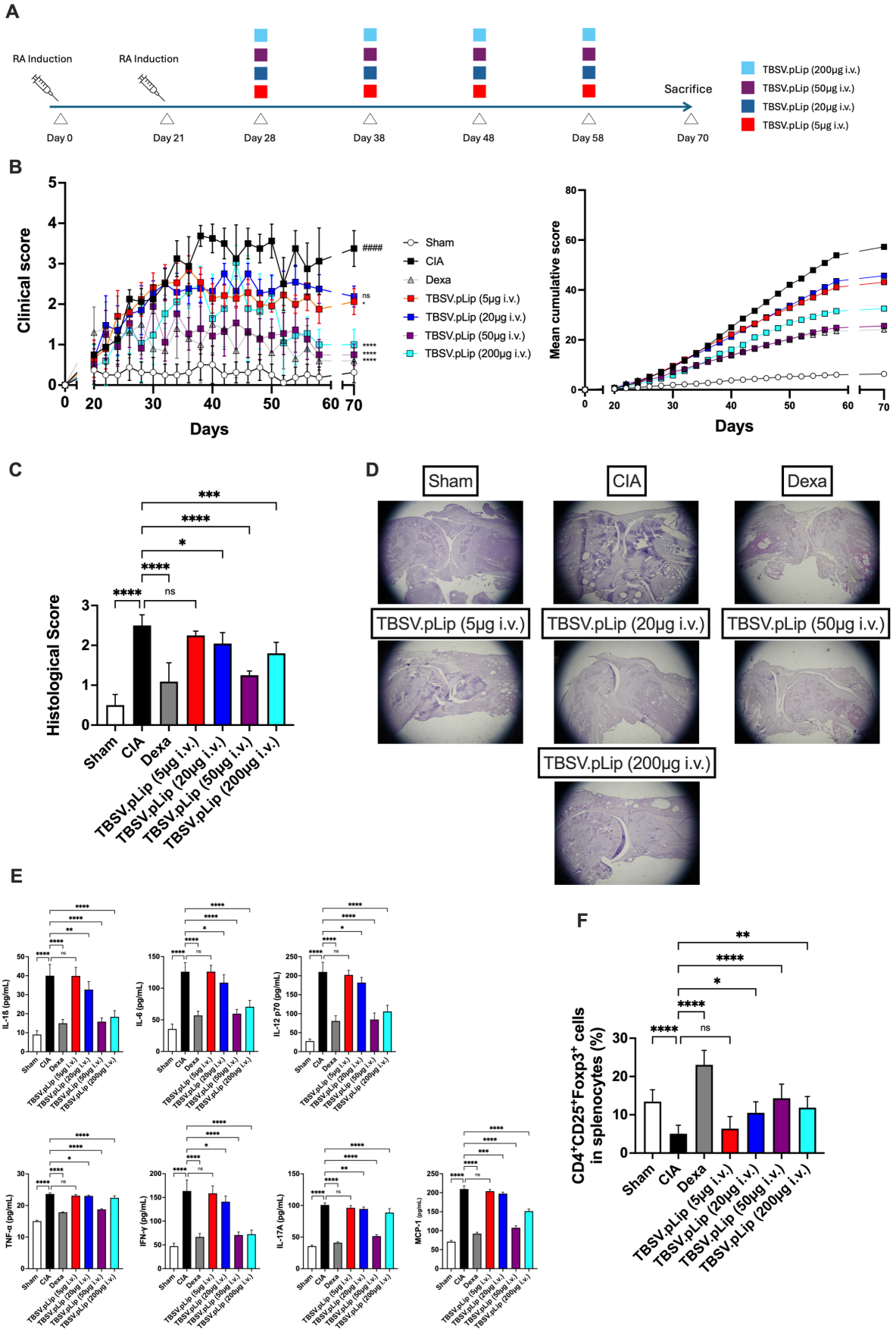
A
RA Induction
RA Induction
Sacrifice
Day 0
Day 21
Day 28
Day 38
Day 48
Day 58
Day 70
TBSV.pLip (200μg i.v.)
TBSV.pLip (50μg i.v.)
TBSV.pLip (20μg i.v.)
TBSV.pLip (5μg i.v.)
B
Clinical score
Days
Sham
CIA
Dexa
TBSV.pLip (5μg i.v.)
TBSV.pLip (20μg i.v.)
TBSV.pLip (50μg i.v.)
TBSV.pLip (200μg i.v.)
Mean cumulative score
Days
C
Histological Score
Sham
CIA
Dexa
TBSV.pLip (5μg i.v.)
TBSV.pLip (20μg i.v.)
TBSV.pLip (50μg i.v.)
TBSV.pLip (200μg i.v.)
D
Sham
CIA
Dexa
TBSV.pLip (5μg i.v.)
TBSV.pLip (20μg i.v.)
TBSV.pLip (50μg i.v.)
TBSV.pLip (200μg i.v.)
E
IL-1β (pg/mL)
IL-6 (pg/mL)
IL-12 p70 (pg/mL)
TNF-α (pg/mL)
IFN-γ (pg/mL)
IL-17A (pg/mL)
MCP-1 (pg/mL)
F
CD4+CD25+Foxp3+ cells in splenocytes (%)
Sham
CIA
Dexa
TBSV.pLip (5μg i.v.)
TBSV.pLip (20μg i.v.)
TBSV.pLip (50μg i.v.)
TBSV.pLip (200μg i.v.)

Figure 6

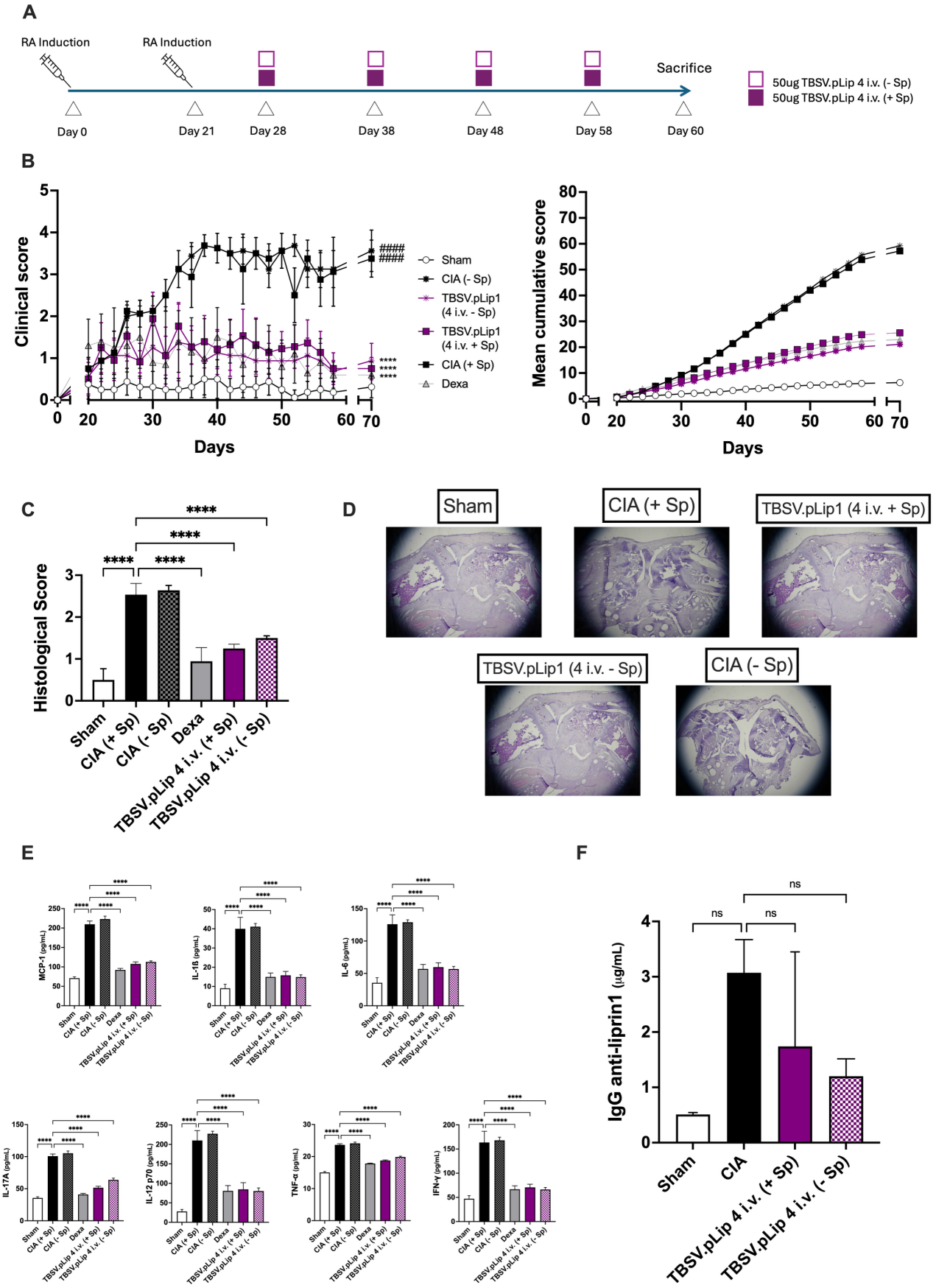
A
RA Induction
RA Induction
Sacrifice
50ug TBSV.pLip 4 i.v. (- Sp)
50ug TBSV.pLip 4 i.v. (+ Sp)
Day 0
Day 21
Day 28
Day 38
Day 48
Day 58
Day 60
B
Clinical score
Days
Sham
CIA (- Sp)
TBSV.pLip1 (4 i.v. - Sp)
TBSV.pLip1 (4 i.v. + Sp)
CIA (+ Sp)
Dexa
Mean cumulative score
Days
C
Histological Score
Sham
CIA (+ Sp)
CIA (- Sp)
Dexa
TBSV.pLip 4 i.v. (+ Sp)
TBSV.pLip 4 i.v. (- Sp)
D
Sham
CIA (+ Sp)
TBSV.pLip1 (4 i.v. + Sp)
TBSV.pLip1 (4 i.v. - Sp)
CIA (- Sp)
E
MCP-1 (pg/mL)
IL-1ß (pg/mL)
IL-6 (pg/mL)
IL-17A (pg/mL)
IL-12 p70 (pg/mL)
TNF-α (pg/mL)
IFN-γ (pg/mL)
F
IgG anti-liprin1 (µg/mL)
ns
Sham
CIA
TBSV.pLip 4 i.v. (+ Sp)
TBSV.pLip 4 i.v. (- Sp)

Figure 7

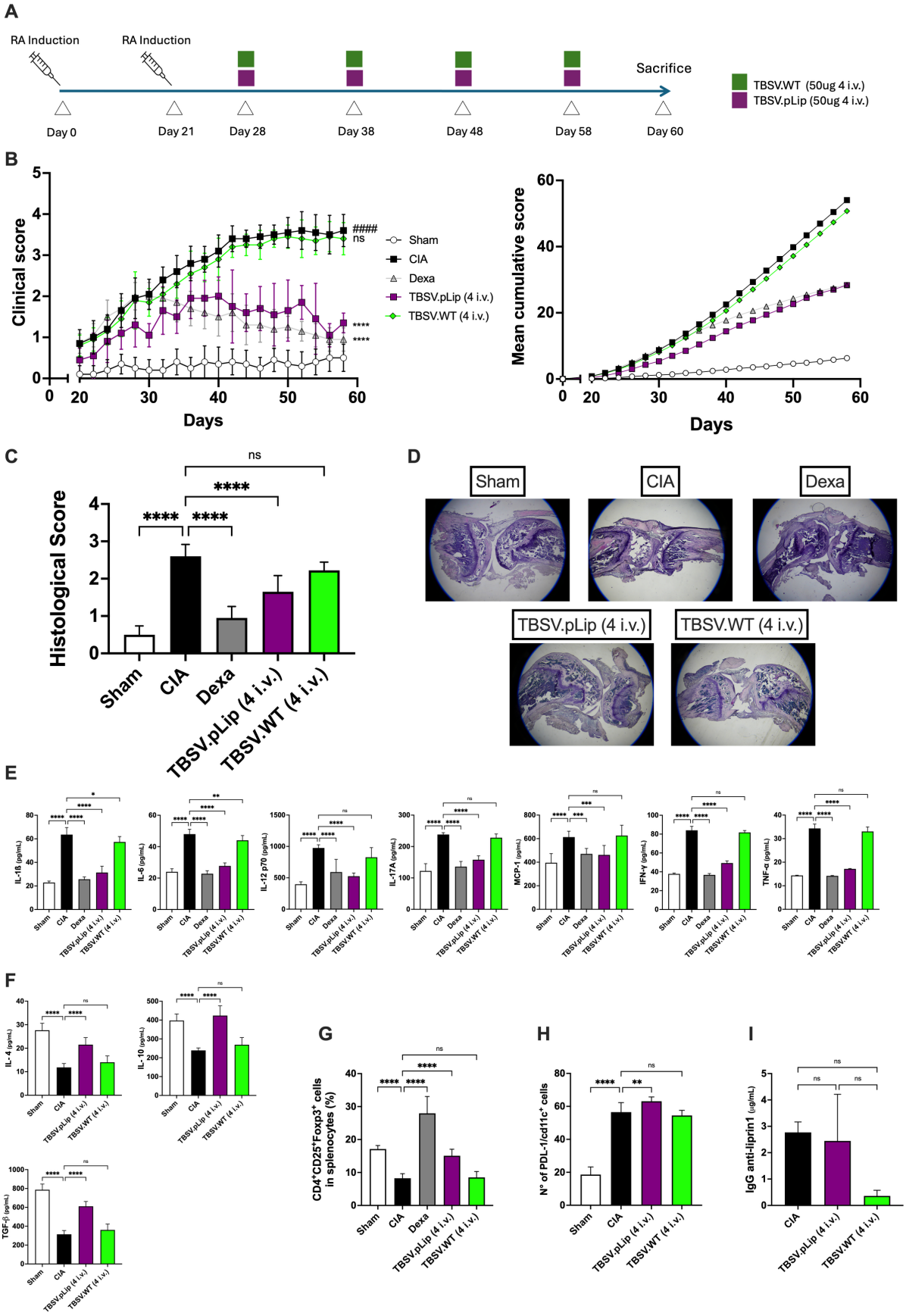
A
RA Induction
RA Induction
Sacrifice
TBSV.WT (50ug 4 i.v.)
TBSV.pLip (50ug 4 i.v.)
Day 0
Day 21
Day 28
Day 38
Day 48
Day 58
Day 60
B
Clinical score
Days
Sham
CIA
Dexa
TBSV.pLip (4 i.v.)
TBSV.WT (4 i.v.)
Mean cumulative score
Days
C
Histological Score
ns
****
Sham
CIA
Dexa
TBSV.pLip (4 i.v.)
TBSV.WT (4 i.v.)
D
Sham
CIA
Dexa
TBSV.pLip (4 i.v.)
TBSV.WT (4 i.v.)
E
IL-18 (pg/mL)
IL-6 (pg/mL)
IL-12 p70 (pg/mL)
IL-17A (pg/mL)
MCP-1 (pg/mL)
IFN-γ (pg/mL)
TNF-α (pg/mL)
F
IL-4 (pg/mL)
IL-10 (pg/mL)
TGF-β (pg/mL)
G
CD4+CD25+Foxp3+ cells in splenocytes (%)
H
N° of PDL-1/cd11c+ cells
I
IgG anti-Liprin1 (µg/mL)

Supplementary Materials

Supplementary Material 1, .csv file containing all the raw data of reported experiments

Supplementary Figure 2

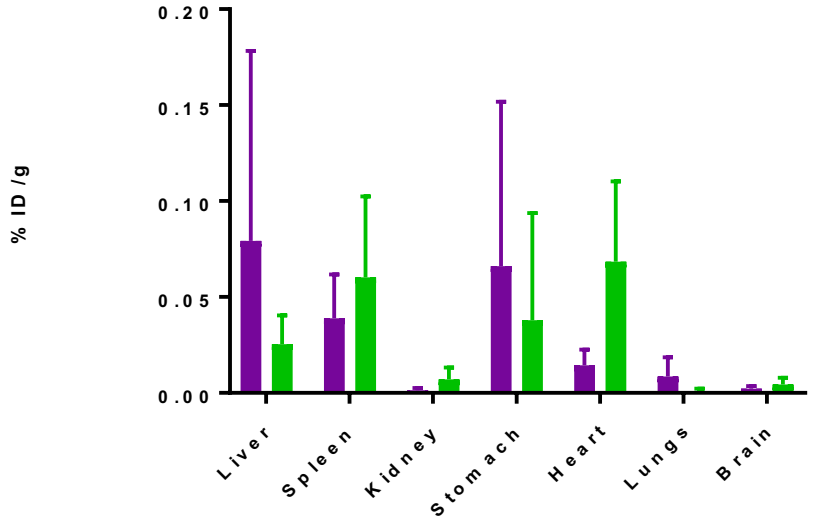

Supplementary Figure 3

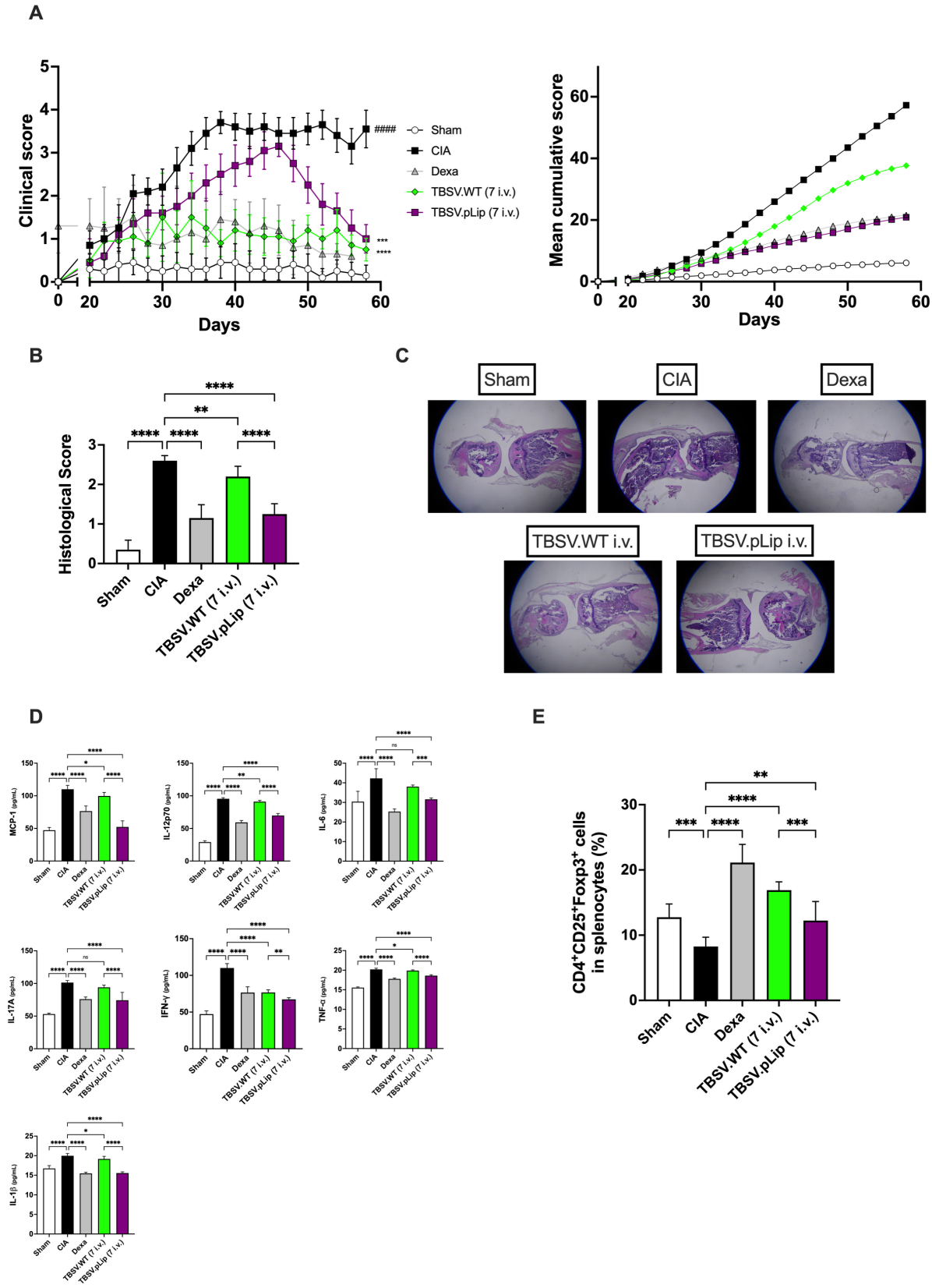

Supplementary Figure 4

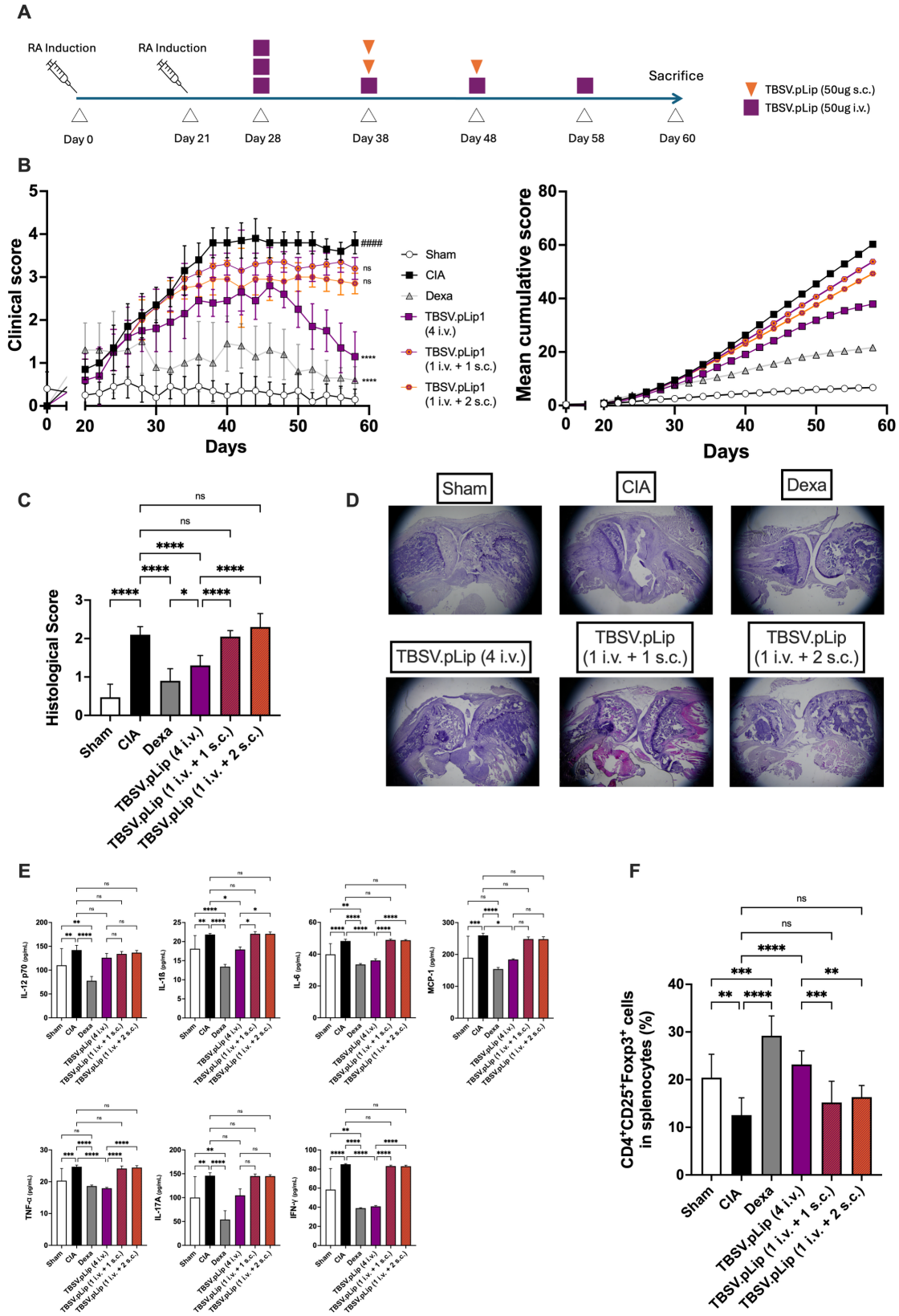
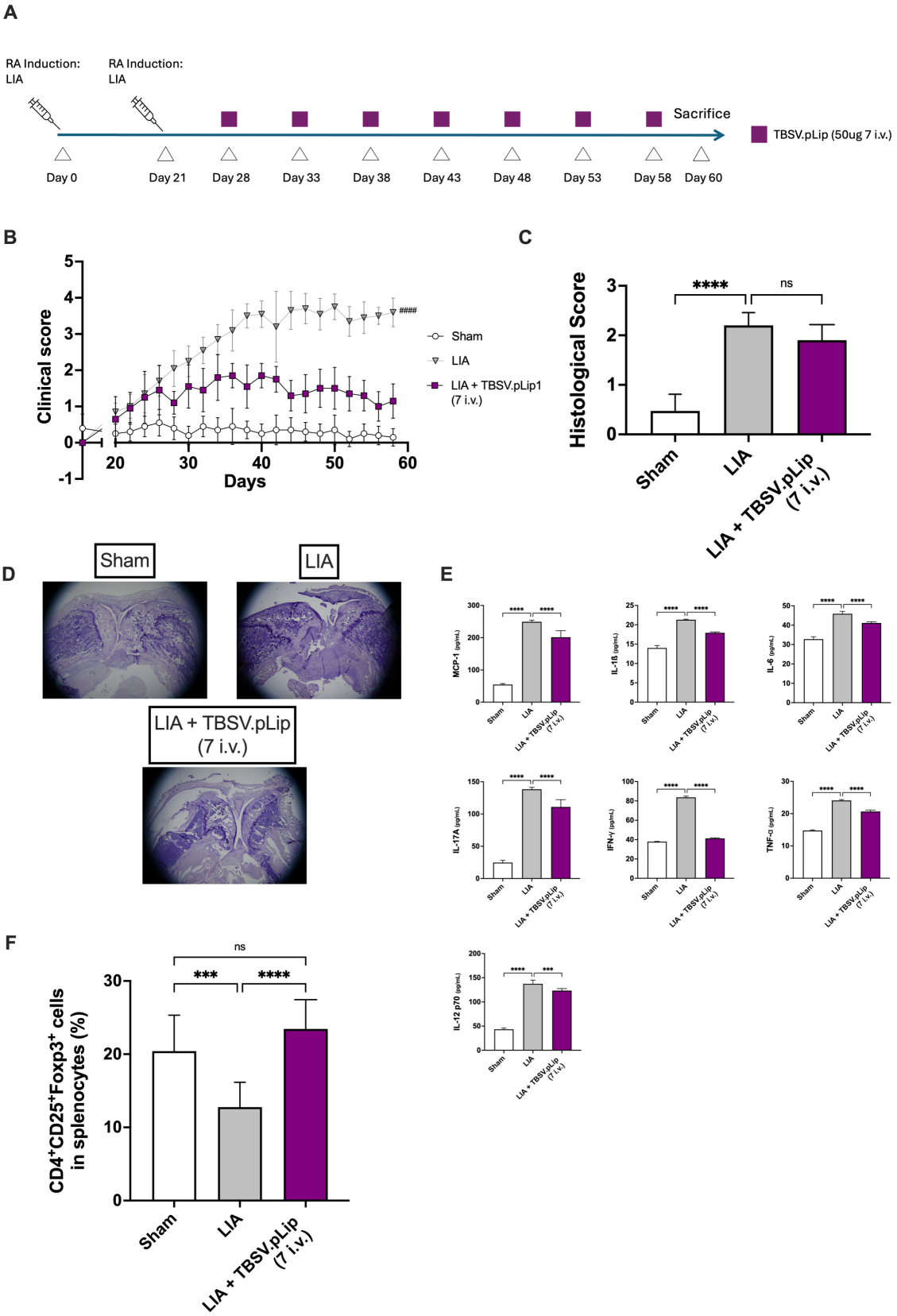
Supplementary Figure 5